

AD

Report DELNV-TR-0031

NEAR INFRARED LASER DYE Q-SWITCHES

by
Carol K. Pearce

May 1982

19970228 061

DTIC QUALITY INSPECTED 2

proved for public release; distribution unlimited.

**U.S. ARMY ELECTRONICS R&D COMMAND
NIGHT VISION & ELECTRO-OPTICS LABORATORY
FT. BELVOIR, VIRGINIA 22060**



**Destroy this report when it is no longer needed.
Do not return it to the originator.**

**The citation in this report of trade names of
commercially available products does not constitute
official endorsement or approval of the use of such
products.**

DISCLAIMER NOTICE



**THIS DOCUMENT IS BEST
QUALITY AVAILABLE. THE
COPY FURNISHED TO DTIC
CONTAINED A SIGNIFICANT
NUMBER OF PAGES WHICH DO
NOT REPRODUCE LEGIBLY.**

UNCLASSIFIED

SECURITY CLASSIFICATION OF THIS PAGE (When Data Entered)

REPORT DOCUMENTATION PAGE		READ INSTRUCTIONS BEFORE COMPLETING FORM
1. REPORT NUMBER DELNV-TR-0031	2. GOVT ACCESSION NO.	3. RECIPIENT'S CATALOG NUMBER
4. TITLE (and Subtitle) NEAR INFRARED LASER DYE Q-SWITCHES		5. TYPE OF REPORT & PERIOD COVERED Technical Report June-December 1979
		6. PERFORMING ORG. REPORT NUMBER
7. AUTHOR(s) Carol K. Pearce		8. CONTRACT OR GRANT NUMBER(s)
9. PERFORMING ORGANIZATION NAME AND ADDRESS USAERADCOM; Night Vision & Electro-Optics Laboratory; Laser Division; Fort Belvoir, VA 22060		10. PROGRAM ELEMENT, PROJECT, TASK AREA & WORK UNIT NUMBERS 1L161102A31B J0 61102A
11. CONTROLLING OFFICE NAME AND ADDRESS USAERADCOM; Night Vision & Electro-Optics Laboratory; Laser Division; Fort Belvoir, VA 22060		12. REPORT DATE May 1982
		13. NUMBER OF PAGES 69
14. MONITORING AGENCY NAME & ADDRESS (if different from Controlling Office)		15. SECURITY CLASS. (of this report) Unclassified
		15a. DECLASSIFICATION/DOWNGRADING SCHEDULE
16. DISTRIBUTION STATEMENT (of this Report) Approved for public release; distribution unlimited.		
17. DISTRIBUTION STATEMENT (of the abstract entered in Block 20, if different from Report)		
18. SUPPLEMENTARY NOTES		
19. KEY WORDS (Continue on reverse side if necessary and identify by block number) Dye Q-Switches Saturable Absorbers Near Infrared Lasers Dyes Dithienes		
20. ABSTRACT (Continue on reverse side if necessary and identify by block number) Fifteen dithiene complexes have been evaluated as near infrared dye Q-switches. Seven of them successfully Q-switched the neodymium 1.06- μ m laser. Optical saturation studies on the dyes are reported and discussed. The high-energy performance of bis (4-dimethylaminiodithiobenzil) nickel is described.		

DD FORM 1473
1 JAN 73

EDITION OF 1 NOV 65 IS OBSOLETE

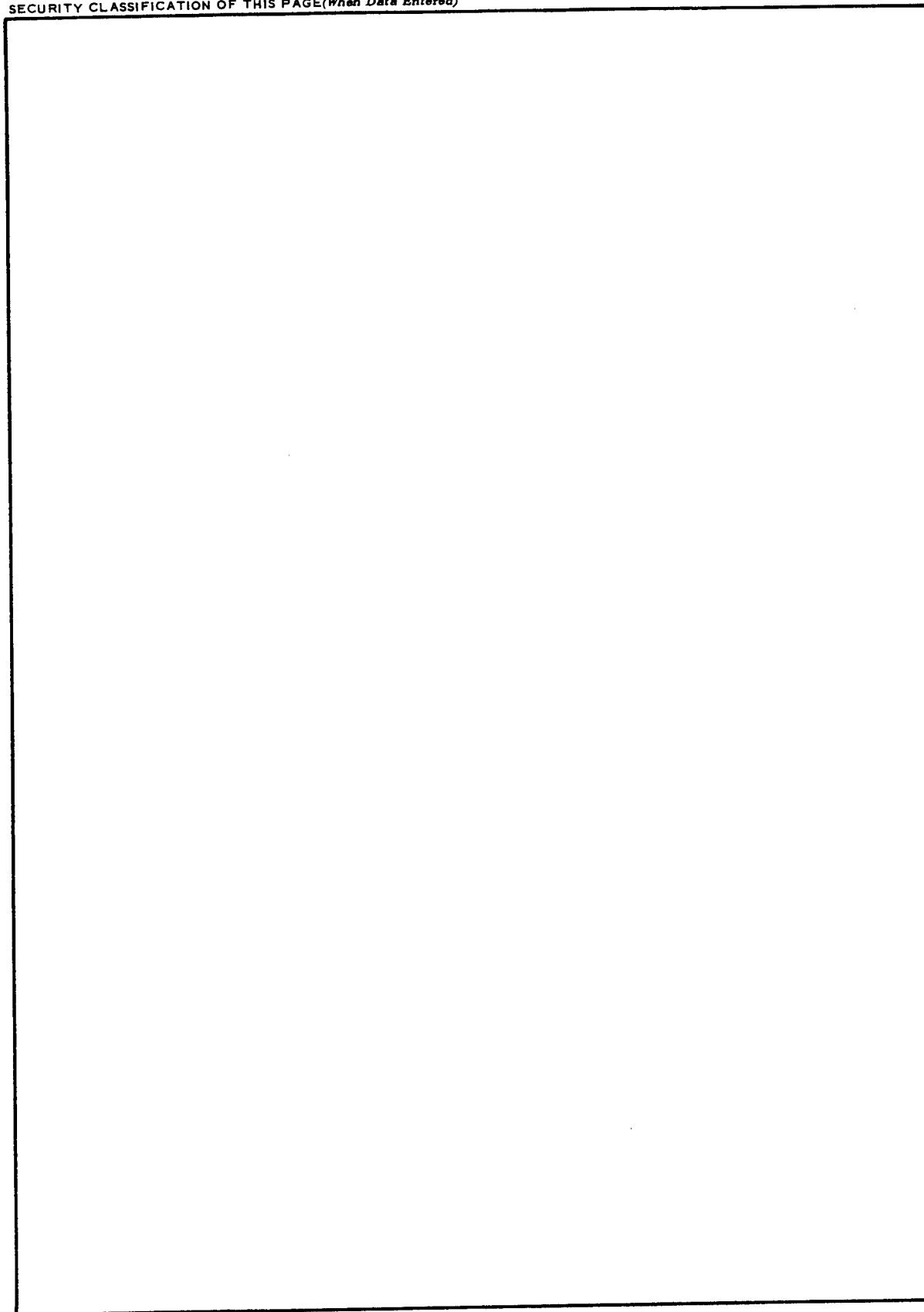
UNCLASSIFIED

i

SECURITY CLASSIFICATION OF THIS PAGE (When Data Entered)

UNCLASSIFIED

SECURITY CLASSIFICATION OF THIS PAGE(When Data Entered)



UNCLASSIFIED

PREFACE

Mr. William Beattie, Laser Division, Night Vision & Electro-Optics Laboratory, assisted in the performance of the laser measurements essential to the research described in this report.

CONTENTS

Section	Title	Page
	PREFACE	iii
	ILLUSTRATIONS	v
	TABLES	viii
I	INTRODUCTION	1
II	EXPERIMENTAL SECTION	
	1. Passive Q-Switch Performance	6
	2. KBr as a Host Medium	26
	3. Optical Saturation Studies	28
	4. Passive Q-Switching of an Nd-Glass Laser for High-Energy Applications	49
III	RESULTS AND DISCUSSION	49
IV	CONCLUSIONS	54

ILLUSTRATIONS

Figure	Title	Page
1	Structural Formula for Ni-DAD (Trans Configuration)	1
2	Simplified Energy Level Diagram for Dye Q-Switch	2
3	Typical Energy Level Diagram Contributing to Intense Infrared Absorption in Dithiene Complexes	5
4	Diagram of Laser Apparatus for Passive Q-Switch Evaluations	6
5	Integrating Circuit for Near Infrared Laser Detector	7
6	Nd:YAG Laser Emission, 1.06 μm	7
7	Absorption Spectrum of Ni-DAD/DCE Solution	12
8	Integrated Energy Trace for Ni-DAD/TCE Solution (1-mm Cell)	13
9	Integrated Energy Trace for Ni-DAD/DCE Solution (1-mm Cell)	13
10	Integrated Energy Trace for Ni-DAD/DCE Solution (1-cm Cell)	14
11	Integrated Energy Trace for Ni-DAD/DCE Solution (1-mm Cell)	14
12	Power Curve for Ni-DAD/DCE Solution (1-mm Cell)	15
13	Integrated Energy Trace for NiTMD/TCE Solution (0.5-cm Cell)	16
14	Integrated Energy Trace for NiTMD/TCE Solution (1-cm Cell)	16
15	Integrated Energy Trace for NiTMD/DCE Solution (1-mm Cell)	17
16	Integrated Energy Trace for NiTMD/DCE Solution (1-cm Cell)	17
17	Power Curve for NiTMD/MS Solution (1-cm Cell)	18
18	Power Curve for NiTMD/DCE Solution (1-mm Cell)	18

ILLUSTRATIONS (CONTINUED)

Figure	Title	Page
19	Power Curve for NiTMD/DCE Solution (1-cm Cell)	19
20	Integrated Energy Trace for PdTMD/DCE Solution (5-mm Cell)	19
21	Power Curve for PdTMD/MS Solution (1-cm Cell)	20
22	Integrated Energy Trace for PtTMD/TCE Solution (1-cm Cell)	21
23	Integrated Energy Trace for PtTMD/DCE Solution (2-cm Cell)	21
24	Integrated Energy Trace for NiODD/CHCl ₃ Solution (1-mm Cell)	22
25	Integrated Energy Trace for NiODD/DCE Solution (5-mm Cell)	22
26	Power Curve for NiODD/DCE Solution (5-mm Cell)	23
27	Integrated Energy Trace for NiOBED/CHCl ₃ (1-mm Cell)	24
28	Integrated Energy Trace for NiMJG/CHCl ₃ (1-cm Cell)	25
29	Integrated Energy Trace for NiTG/CHCl ₃ (1-mm Cell)	25
30	Integrated Energy Trace for NiDMI/CHCl ₃ (1-mm Cell)	27
31	Integrated Energy Trace for NiDMI/CHCl ₃ (1-mm Cell)	27
32	Experimental Configuration for Optical Saturation Studies	30
33	Optical Saturation of EK No. 9740/Chlorobenzene Solution	31
34	Optical Saturation of EK No. 9860/DCE Solution	32
35	Optical Saturation of BFCO ₂ PF ₆ /Benzonitrile Solution	33
36	Optical Saturation of Ni-DAD/DCE Solution	34
37	Optical Saturation of NiTG/CHCl ₃ Solution	35

ILLUSTRATIONS (CONTINUED)

Figure	Title	Page
38	Optical Saturation of NiI/CHCl ₃ Solution	36
39	Optical Saturation of NiODD/CHCl ₃ Solution	37
40	Optical Saturation of NiMJG/CHCl ₃ Solution	38
41	Optical Saturation of NiOBED/CHCl ₃ Solution	39
42	Optical Saturation of NiOMeS/DCE Solution	40
43	Optical Saturation of NiDMI/CHCl ₃ Solution	41
44	Optical Saturation of NiD/CHCl ₃ Solution	42
45	Optical Saturation of NiDTPQ/DMF Solution	43
46	Optical Saturation of NiDTAQ/DMF Solution	44
47	Optical Saturation of NiTMD/DCE Solution	45
48	Optical Saturation of PdTMD/DCE Solution	46
49	Optical Saturation of PtTMD/DCE Solution	47
50	Optical Saturation of NiDJG/DCE Solution	48
51	Diagram of Apparatus Used to Generate and Measure High-Energy 1.06 μ m Laser Emission	50
52	Apparent Plateau of Ni-DAD Response	51

TABLES

Table	Title	Page
1	Diethiene Complexes as Candidate Passive Absorbers at 1.06 μm	9
2	High-Energy Performance of Ni-DAD	11

NEAR INFRARED LASER DYE Q-SWITCHES

I. INTRODUCTION

Passive Q-switching of Nd ($1.06\ \mu\text{m}$) lasers has been achieved successfully, to the extent that at least four Q-switch dyes are available commercially.¹ Of these four, two are of the cyanine class and are susceptible to photochemical degradation. The other two, bis (4-dimethylaminodithiobenzil) nickel (hereafter Ni-DAD) and bis (4-diethylaminodithiobenzil) nickel (hereafter Ni-DEAD) are dithiene complexes of nickel (Figure 1) and exhibit a high degree of photochemical stability. No dye Q-switches are known at present for lasers operating in the near infrared at longer wavelengths than $1.06\ \mu\text{m}$, however. Among the advantages of a dye Q-switch are its simplicity, light weight, and low cost compared to other laser Q-switches. Incorporation of the Q-switch dye, Ni-DAD, in a plastic host, in the ANG PVS-5 and 6 rangefinders, and in the PVQ-3 Grenade Launcher clearly demonstrated these advantages.²

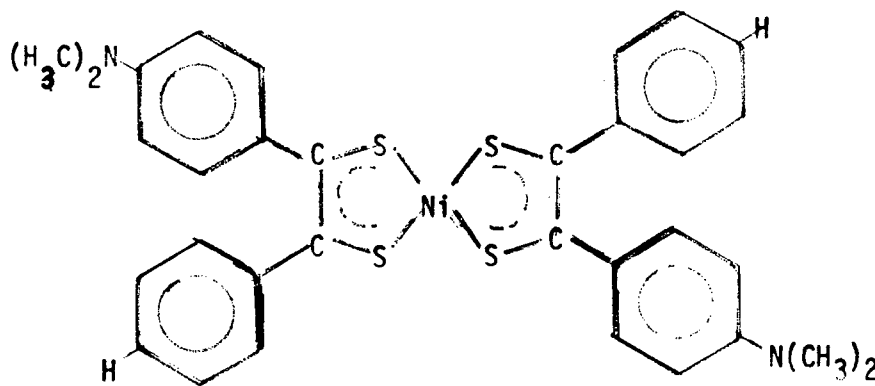


Figure 1. Structural formula for Ni-DAD (trans configuration).

¹ "Eastman Laser Dyes," Eastman Publication JJ-169, Eastman Kodak Co., pp 19-21 (1977).

² J. Strozyk, "A Performance Evaluation of Mini-Laser Cartridge Devices," US Army ERADCOM Technical Report (April 1979).

The fundamental mechanism for a dye Q-switch is absorption (of the laser emission) by dye molecules in their ground state, with subsequent transitions to excited levels which are transparent to the laser wavelength. When the population in this state becomes high enough, the characteristic Q-switched giant pulse is obtained. Figure 2 depicts an appropriate generalized energy level diagram for a dye Q-switch.

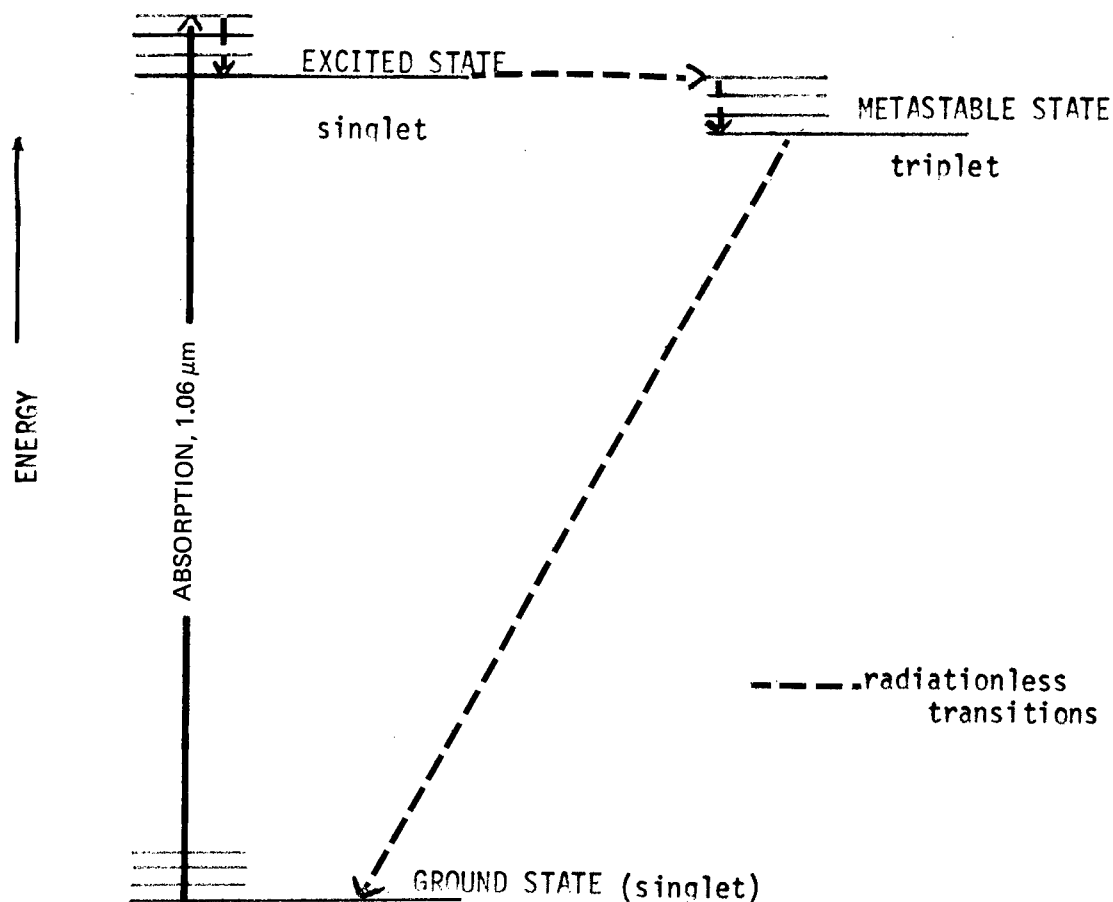


Figure 2. Simplified energy level diagram for dye Q-switch.

Work with dye Q-switches at other wavelengths, especially in the visible, has established certain fundamental criteria for a dye to be a successful laser Q-switch, namely:

- a. A light absorption maxima at the wavelength of the laser emission.
- b. An extinction coefficient ϵ , of about $10^4 \text{ l-mol}^{-1}\text{-cm}^{-1}$, or greater.³
- c. Sufficiently long decay times for the excited state, so that a significant population of molecules is present in that state.
- d. Photochemical stability.

An extensive search of the literature produced negligible evidence of compounds known to satisfy even the first two criteria at near infrared wavelengths longer than $1.06 \mu\text{m}$. Either an extensive effort would be required to record and analyze the near-infrared spectra of known compounds, or candidate dye Q-switches would have to be identified through empirical and theoretical approaches. Efficiency demanded an empirical approach, supported by theoretical concepts.

³ The molar extinction coefficient ϵ is related to the absorbance, $\log I_0/I$, by the Beer-Lambert Law:

$$\log \frac{I_0}{I} = \epsilon \cdot l \cdot c$$

where I_0 is the incident light intensity upon an absorber whose path length is 1 cm, the absorber concentration being c moles/liter. I is the intensity of light exiting from the cell.

The molecular absorption cross section σ results when the concentration is C molecules/cc:

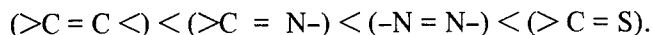
$$\ln \frac{I_0}{I} = \sigma CL$$

The relationship between ϵ and σ , when Avogadro's number, N_a , is 6.02×10^{23} molecules per mole is:

$$\epsilon = \frac{N_a \sigma}{2303}$$

The value of ϵ at the wavelength of maximum absorption is ϵ_{max} .

Treating the passive absorber as a dye or an "auxochromophoric system," one finds certain molecular compositions and configurations will favor extension of absorption maxima towards longer wavelengths.^{4,5} Incorporation of certain structures or groups into the molecules can contribute the presence of highly mobile electrons that are free to travel over extended resonance paths thus enhancing the red (bathochromic) shift. Absorption is found to shift to longer wavelengths to an increasing extent according to the presence of such unsaturated linkages as:⁴



Extended resonance paths can be achieved by increasing the extent of conjugated unsaturated linkages, particularly in a planar configuration.^{4,5}

Only the first two criteria noted earlier will benefit from consideration of the traditional concepts of dye absorption maxima. The third criterion, that of decay or relaxation times, is less easily approached. Precise experimental measurements are complex, and even for known dye candidates, values are not readily available from previous work. The best first approximation that can be made to satisfy all four criteria is to consider modifications of known successful near infrared dye Q-switches. The highly stable dithiene Q-switches Ni-DAD and Ni-DEAD are characterized by the ($>C = S$) linkage. Molecular engineering can be applied to create new dithienes with extended resonance paths. This is the approach used in the work reported below on dithiene derivatives.

The Q-switches, Ni-DAD and Ni-DEAD, are derivatives of the planar, monomeric, neutral nickel complex, bisdithioglyoxal-nickel or $Ni-S_4C_4H_4$. Analysis of the electronic spectrum of the latter compound led to the conclusion that the intense absorption around $1\ \mu m$ that is of interest to us is the result of an allowed $\pi - \pi^*$ transition between the $2b_{1u}$ and the $3b_{2g}$ levels of the complex (Figure 3).^{6,7,8} This transition was found to be highly sensitive to substituents on the ligand of the complex, making these dithiene complexes promising candidates for a molecular engineering approach to achieve near infrared Q-switches. The success of Ni-DAD has been noted already.^{9,10}

⁴ L. Fieser and M. Fieser, *Organic Chemistry*, D.C. Heath and Co., Boston, Chap. 34 (1944).

⁵ K. Venkataraman, *The Chemistry of Synthetic Dyes*, Vol I, Academic Press Inc., New York NY, Chap. VIII (1952).

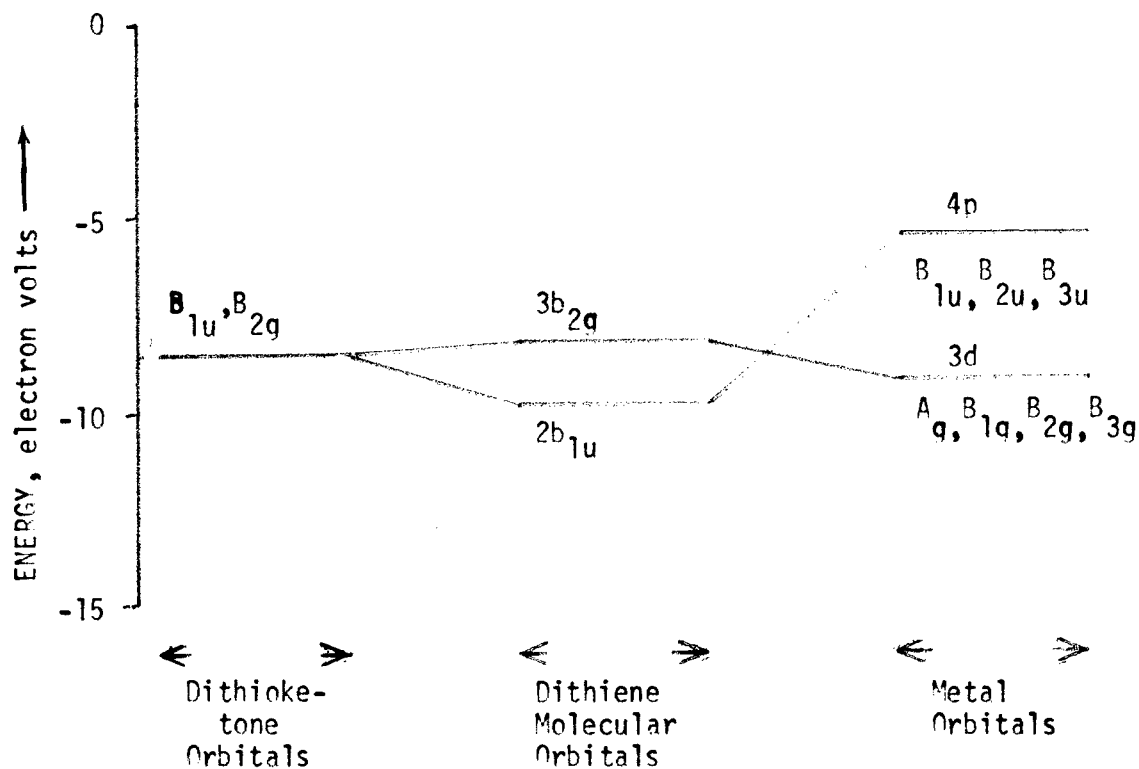
⁶ G. N. Schrauzer and V. P. Mayweg, *J.A.C.S.* 87(1), 3585 (1965).

⁷ G. N. Schrauzer, *Accts. Chem. Res.* 2(3), 72 (1969).

⁸ D. Magde, B. A. Bushaw, and M. W. Windsor, *Chem. Phys. Ltrs.* 28(2), 263 (1974).

⁹ K. H. Drexhage and U. T. Muller-Westerhoff, *IEEE J. of QE*, QE-8(9), 759 (1972).

¹⁰ H. Lo, "Saturable Absorbing Materials for Q-Switching Neodymium Lasers," ECOM Research and Development Report ECOM-0122-F (May 1972).



Molecular orbital energy levels, for the complex $Ni(C_2H_2S_2)_2$, contributing to the intense near infrared absorption typical of the dithienes.⁷ The energy levels for the Ni-DAD dye, $Ni(S_2C_2(C_6H_5)(C_6H_4)N(CH_3)_2)_2$, would be similar to this, but would be affected by the increased substitution in the dithiene ligand.

Figure 3. Typical energy level diagram contributing to intense infrared absorption in dithiene complexes.

⁷ G. N. Schrauzer, *Accts. Chem. Res.* 2(3), 72 (1969).

II. EXPERIMENTAL SECTION

1. Passive Q-Switch Performance.

a. **Experimental Apparatus.** Q-switch evaluations were made in the apparatus diagrammed in Figure 4, the lasing element being a $\frac{1}{4}$ -in. OD x $2\frac{1}{2}$ -in. Nd:YAG rod with parallel faces. Operating at 10 p/s, this laser emitted a 100-mJ long pulse. A silicon SD100 detector was used to monitor the integrated pulses for single pulsing, and a Texas Instruments germanium avalanche detector with 50-ohm load was used for the power pulse traces. Oscilloscopes used with the detectors were Tektronix type 564B with the SD100 detector and type 485 with the avalanche detector. Some Q-switch evaluations were done using an erbium silicate glass laser, using both the SD100 and germanium avalanche detectors.¹¹ Alignment techniques were those used conventionally in this laboratory.¹¹ During earlier Q-switch investigations in this laboratory, a technique was developed to integrate the energy of a pulse so that the oscilloscope display clearly indicated whether single or multiple pulsing is occurring.¹² This technique was applied in the present work. The integrating circuit is shown in Figure 5, and a typical oscilloscope tracing is that of Figure 6 for the long pulse of the neodymium-YAG laser. Variable energy of the laser pulse, as well as dye concentration, affected the Q-switched output.

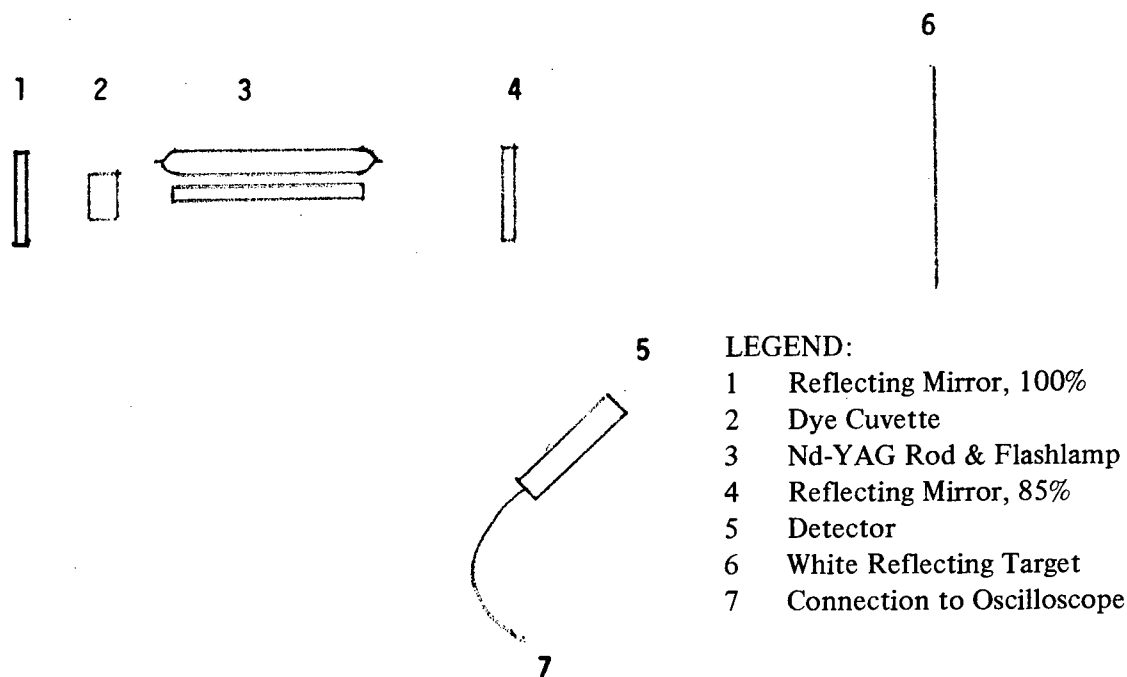


Figure 4. Diagram of laser apparatus for passive Q-switch evaluations.

¹¹ J. M. Strok, W. C. Beattie, and E. J. Tebo, "Erbium Laser Rangefinding," US Army Research and Development Report ECOM 3582 (June 1972).

¹² W. C. Beattie, US Army (ERADCOM) private communication.

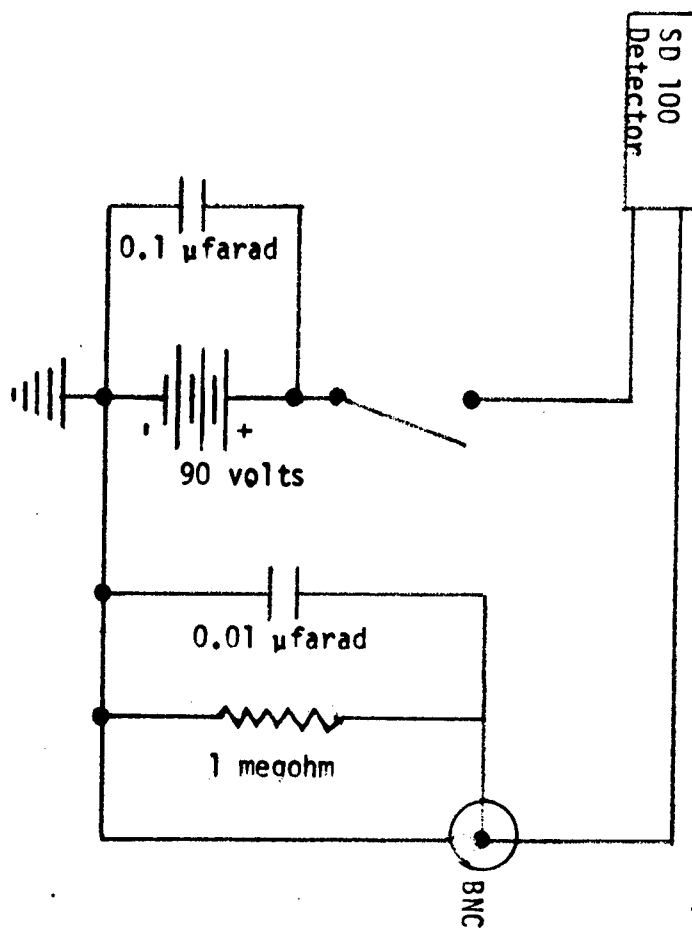
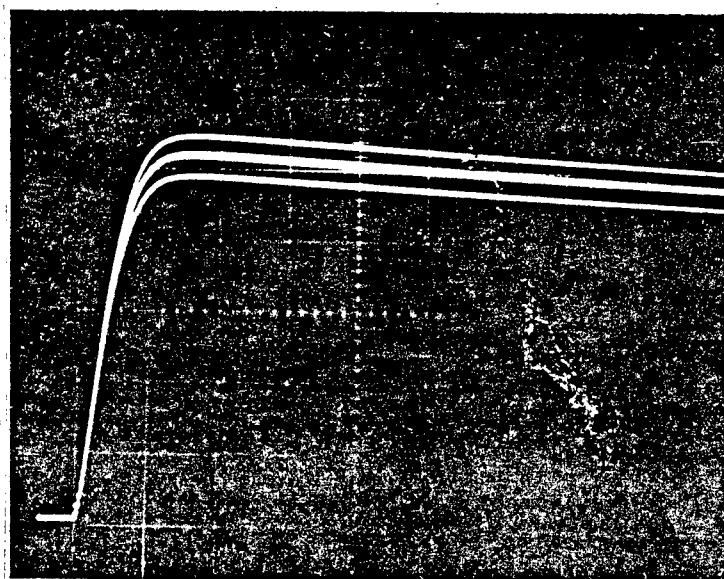


Figure 5. Integrating circuit for near infrared laser detector.

OSCILLOSCOPE RESPONSE

200 MILLIVOLTS/CM



50 MICROSECONDS/CM

SWEEP SPEED

Figure 6. Nd:YAG laser emission, 1.06 μm.

Spectral absorption measurements were made on a Cary Recording Spectrophotometer Model 14. Cylindrical absorption cells made from near IR transmitting silica were used for these measurements and for Q-switch tests. Path lengths of 1 mm, 2 mm, 5 mm, or 1 cm were used. The dithiene complexes used are shown in Table 1. The materials were used as received from the source indicated, without further purification.^{13 14} Ni-DAD was obtained from Eastman Kodak Co. The dyes were used in approximately 10^{-4} M solutions for Q-switch testing. The solvents used to prepare the dye solutions were tetrachloroethylene (TCE) (Eastman Spectro Grade), methyl sulfoxide (MS) (Eastman Spectro grade), 1,2-dichloroethane (DCE) (Eastman Spectro Grade), chloroform (CHCl_3) (Fisher Spectro-analyzed Grade), pyridine (Py) (MC/B Spectroquality Grade), and dimethylformamide (DMF) (Fisher Certified Grade).

b. Experimental Results. The Q-switch evaluations for each of the compounds shown in Table 1 are presented below. Pertinent light absorption data are summarized in Table 2. The absorption spectrum for Ni-DAD is shown in Figure 7 and is typical for the other complexes except for the position of the maximum.

Ni-DAD (4-dimethylaminodithiobenzil) nickel). Ni-DAD was studied in three solvents, TCE, DCE, and MS, yielding pale green solutions. As noted before, it is well known as a passive Q-switch for the neodymium $1.06 \mu\text{m}$ laser.^{9 10} In DCE, ϵ_{max} has been determined to be $2.5 \times 10^4 \text{ l-mol}^{-1}\text{-cm}^{-1}$.⁹ The absorption maximum was at $1.06 \mu\text{m}$ in each of the three solvents. Integrated energy traces are presented in Figures 8 through 11, and a power curve is shown in Figure 12. Evidence for mode-locking was found when methyl sulfoxide was the solvent.

Ni-D (bis-(dithiobenzil)-nickel). This compound is similar to Ni-DAD except that the phenyl rings are unsubstituted. Only the emerald green chloroform solution was studied. With an absorption maximum at 850 nm , its failure to Q-switch the Nd ($1.06 \mu\text{m}$) laser is understandable. In CHCl_3 , ϵ_{max} was found to be $2.71 \times 10^4 \text{ l-mol}^{-1}\text{-cm}^{-1}$.

⁹ K. H. Drexhage and U. T. Muller-Westerhoff, IEEE J. of QE, QE-8 (9), 759 (1972).

¹⁰ H. Lo, "Saturable Absorbing Materials for Q-switching Neodymium Lasers," ECOM Research and Development Report ECOM-0122-F (May 1972).

¹³ A. Nazzari, R. Lane, J. Mayerle, and U. T. Mueller-Westerhoff, "The Synthesis of Substituted Nickel Dithiene Complexes with Intense Electronic Transitions in the Infrared Region," AD-A054675, Defense Documentation Center, Alexandria, VA (April 1978).

¹⁴ C. Snyder, IBM Corp., private communication.

Table 1. Dithiene Complexes as Candidate Passive Absorbers at 1.06 μm

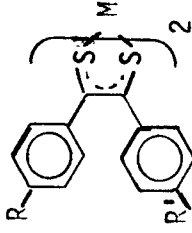
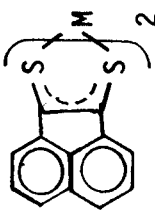
Basic Molecule	R	R'	M	Symbol	Absorption Max μm	Molar Absorptivity $\text{ex}10^{-4}$ max	Nd Laser Q-Switch Performance	Opening at 1 MW
	-H	-H	Ni	NiD	0.850	2.98	No	No
	$-\text{N}(\text{CH}_3)_2$	-H	Ni	NiDAD	1.06	2.5	Excellent	Yes
	$-\text{OCH}_3$	$-\text{OCH}_3$	Ni	NiTMD	0.925	3.2	Low-energy pulse	Slight
	$-\text{OCH}_3$	$-\text{OCH}_3$	Pd	PdTMD	0.950	4.1	Mode-locks	Slight
	$-\text{OCH}_3$	$-\text{OCH}_3$	Pt	PtTMD	0.860	4.2	No	No
	$-\text{OC}_{10}\text{H}_{24}$	$-\text{OC}_{10}\text{H}_{21}$	Ni	NiODD	0.935	3.4	High-energy stable	Yes
	$-\text{OCH}_2\text{CO}_2\text{K}$	$-\text{OCH}_2\text{CO}_2\text{K}$	Ni	NiOCKD	0.920	1.8	No	Not examined
	$-\text{OCH}_2\text{CO}_2\text{CH}_3$	$-\text{OCH}_2\text{CO}_2\text{CH}_3$	Ni	NiOMESD	0.920	2.7	No	No
	$-\text{O}(\text{CH}_2)_3\text{CO}_2\text{C}_2\text{H}_5$	$-\text{O}(\text{CH}_2)_3\text{CO}_2\text{C}_2\text{H}_5$	Ni	NiOBED	0.925	3.2	Variable	Yes
	-H	-H	Ni	NiDTAQ	1.14	Not determined	No	No
								

Table 1. Dithiene Complexes as Candidate Passive Absorbers at 1.06 μm (Continued)

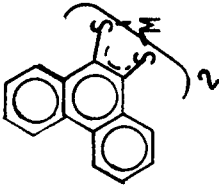

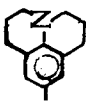
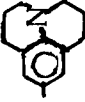



Basic Molecule	R	R'	M	Symbol	Absorption		Molar Absorptivity $\times 10^{-4}$ max	Nd Laser Q-Switch Performance	Opening at 1 MW
					Max μm	λ max			
	-H	-H	Ni	NIDTPQ	1.01		Not determined	No	No
									
		-H	Ni	NIMJG	1.155		0.99	Mod. energy	Yes
			Ni	NIDJG	1.28		2.0	No	No
	-H	-H	Ni	NITG	0.908		2.0	Low energy	Yes
	-H	-H	Ni	NII	0.90		1.1	No single pulsing; very low energy double pulsing	Yes
	-N(CH ₃) ₂	-H	Ni	NIDMI	1.05		0.5	Variable, low energy	No

Table 2. High-Energy Performance of Ni-DAD
(Nd silicate glass laser unless otherwise specified.)

Giant Pulse Output, Joules		Long Pulse Output, Joules (Non-Q- Switched Pulse)	Absorbance Ni-DAD Dye Q-Switch	Efficiency of Q-Switching	Percent Reflectivity of Front Mirror
Ni-DAD Dye Q- Switch	KD*P Pockels Cell Q-Switch				
0.63		3.4	0.335	18.5	75
0.69		4.6	0.335	15.0	50
0.77		5.4	0.360	14.3	50
	1.15 (Nd phosphate Glass Rod)	2.9		39.7	50-75
0.081		0.203	0.270	39.9	85

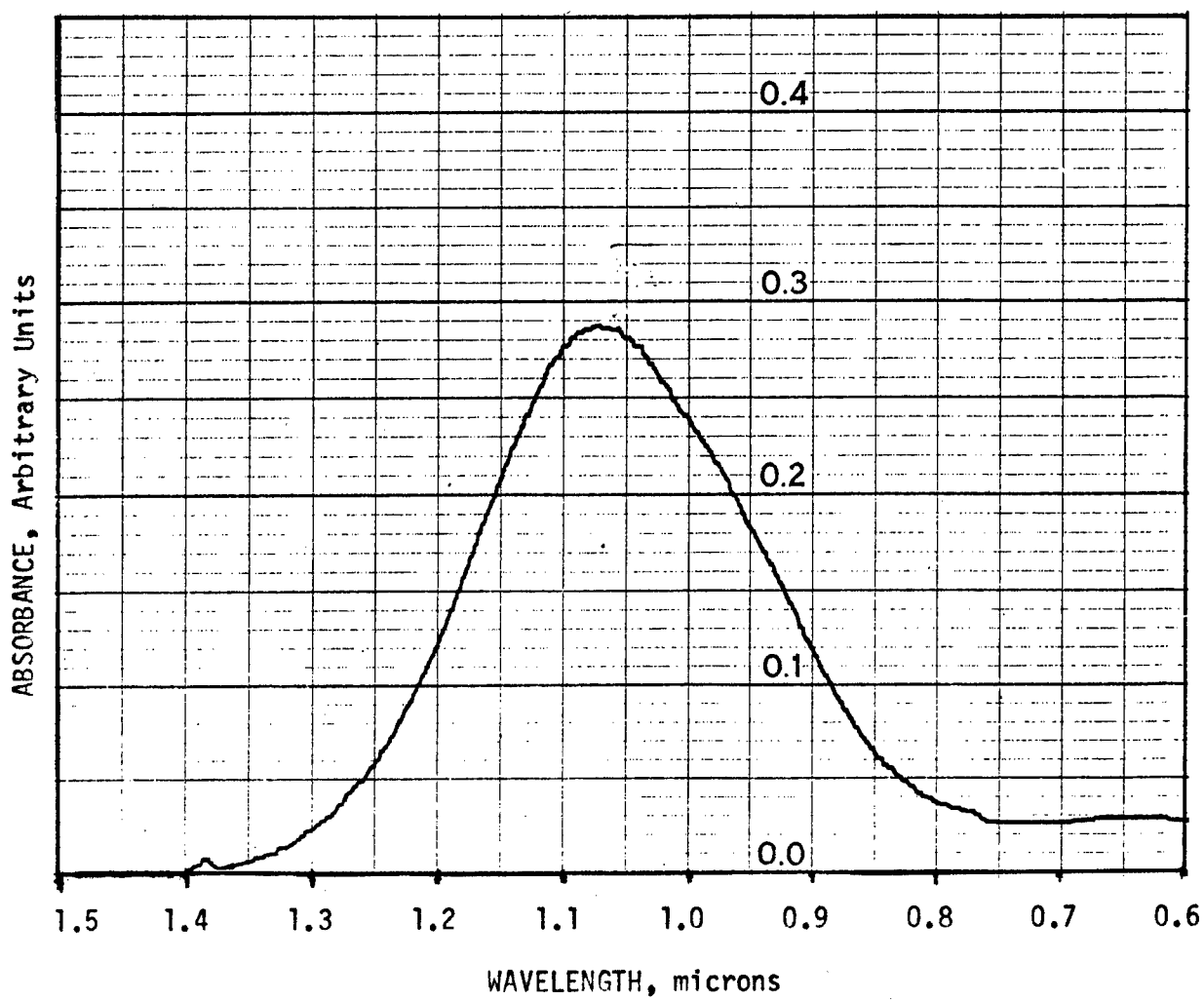
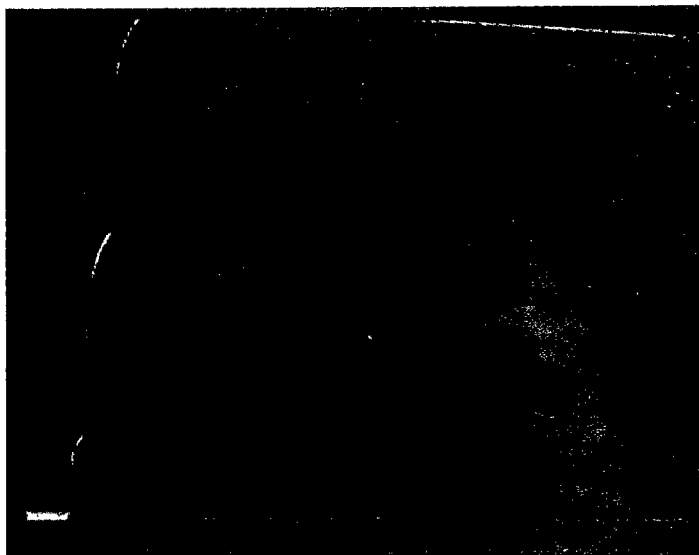


Figure 7. Absorption spectrum of Ni-DAD/DCE solution.

OSCILLOSCOPE RESPONSE

20 MILLIVOLTS/CM



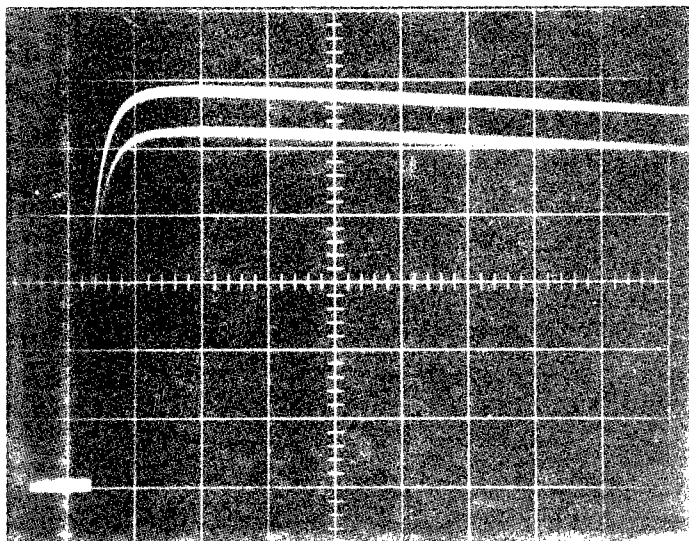
50 MICROSECONDS/CM

SWEEP SPEED

Figure 8. Integrated energy trace for Ni-DAD/TCE solution (1-mm cell).

OSCILLOSCOPE RESPONSE

10 MILLIVOLTS/CM



50 MICROSECONDS/CM

SWEEP SPEED

Figure 9. Integrated energy trace for Ni-DAD/DCE solution (1-mm cell).

OSCILLOSCOPE RESPONSE

100 MILLIVOLTS/CM



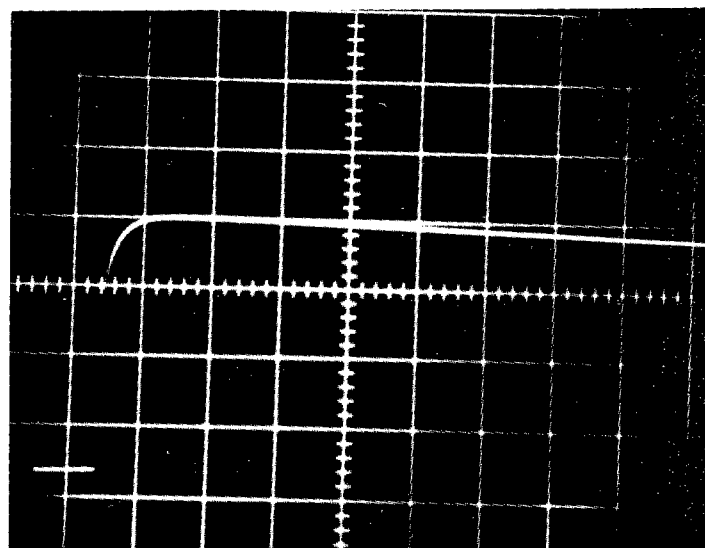
50 MICROSECONDS/CM

SWEEP SPEED

Figure 10. Integrated energy trace for Ni-DAD/DCE solution (1-cm cell).

OSCILLOSCOPE RESPONSE

50 MILLIVOLTS/CM



50 MICROSECONDS/CM

SWEEP SPEED

Figure 11. Integrated energy trace for Ni-DAD/DCE solution (1-mm cell).

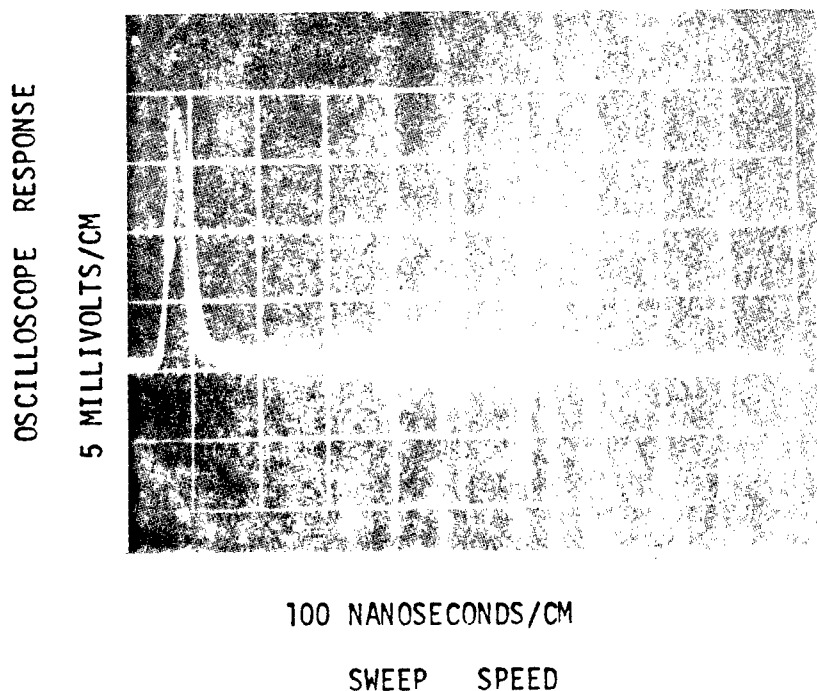


Figure 12. Power curve for Ni-DAD/DCE solution (1-mm cell).

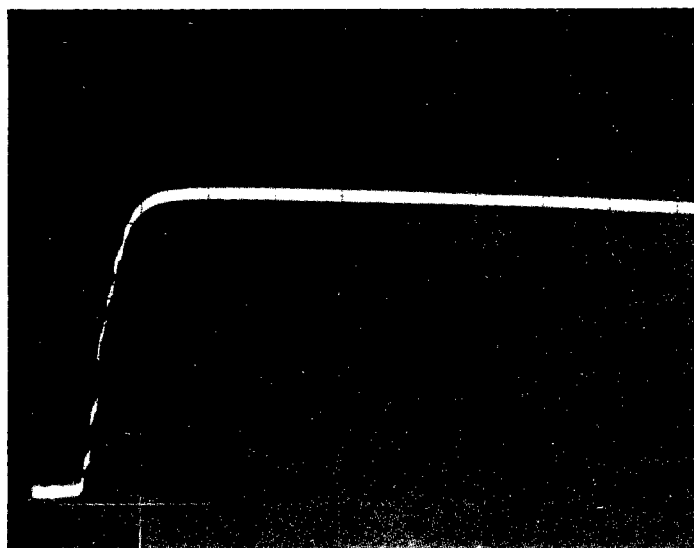
Ni-TMD (bis(4,4'-dimethoxydithiobenzil)-nickel). Ni-TMD solutions were prepared in TCE, DCE, and MS, the latter two affording good solubility. The absorption maximum ranged from 925 nm to 950 nm. In DCE, the absorption maximum was at 930 nm, with $\epsilon_{\text{max}} = 3.2 \times 10^4 \text{ l-mol}^{-1}\text{-cm}^{-1}$.

The integrated energy curves of Figures 13 through 16 show that the compound will Q-switch the Nd laser and mode-locks in methyl sulfoxide (Figure 17). The energy is somewhat attenuated when a single pulse is achieved, however. Power curves are shown in Figures 18 and 19.

Pd-TMD (bis(4,4'-dimethoxydithiobenzil)-palladium). Solutions were prepared in TCE, DCE, and MS, as in the previous case. Solubility results were similar to those for the nickel complex, but rose pink solutions formed. Absorption spectra indicate absorption maxima around 950 nm. A few low-energy pulses occurred in DCE, with mode-locking in MS (Figures 20 and 21). Only attenuation occurred in TCE. At the absorption maximum of 950 nm in DCE, ϵ_{max} was $4.1 \times 10^4 \text{ l-mol}^{-1}\text{-cm}^{-1}$.

OSCILLOSCOPE RESPONSE

10 MILLIVOLTS/CM



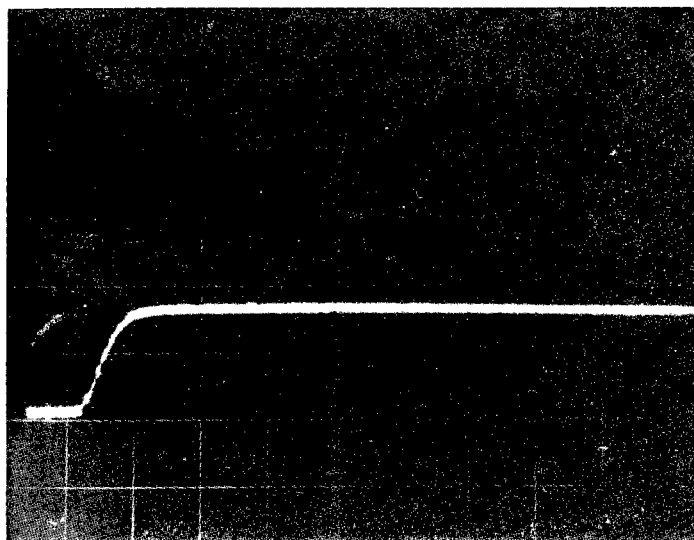
50 MICROSECONDS/CM

SWEEP SPEED

Figure 13. Integrated energy trace for NiTMD/TCE solution (0.5-cm cell).

OSCILLOSCOPE RESPONSE

10 MILLIVOLTS/CM

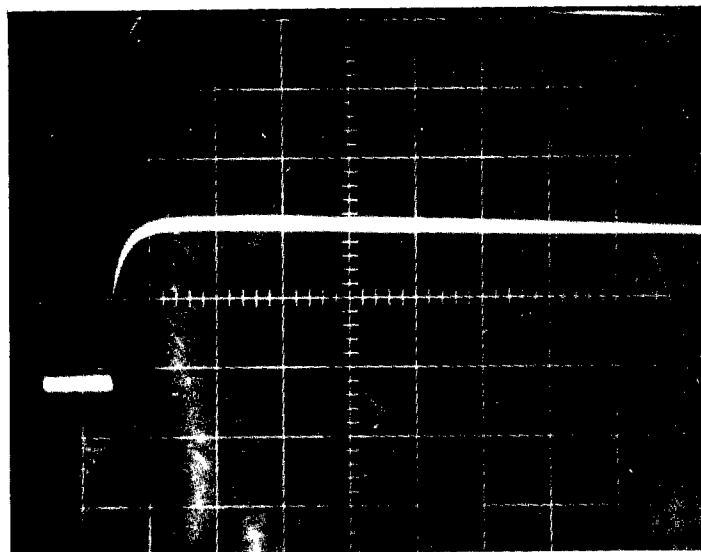


50 MICROSECONDS/CM

SWEEP SPEED

Figure 14. Integrated energy trace for NiTMD/TCE solution (1-cm cell).

OSCILLOSCOPE RESPONSE
10 MILLIVOLTS/CM

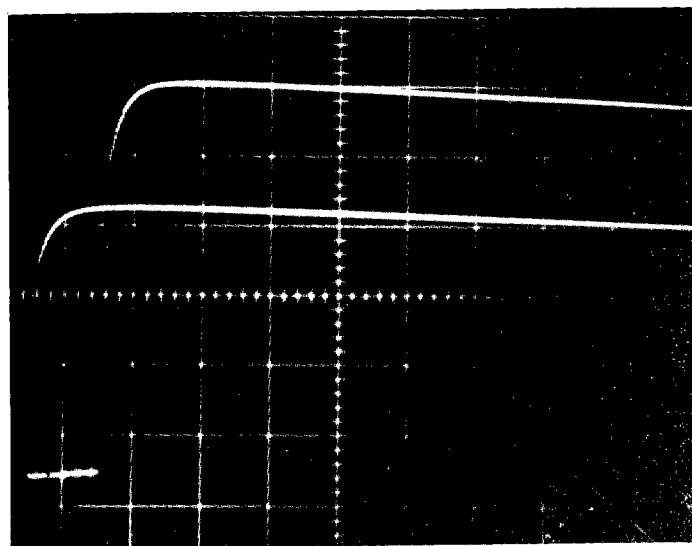


50 MICROSECONDS/CM

SWEEP SPEED

Figure 15. Integrated energy trace for NiTMD/DCE solution (1-mm cell).

OSCILLOSCOPE RESPONSE
10 MILLIVOLTS/CM



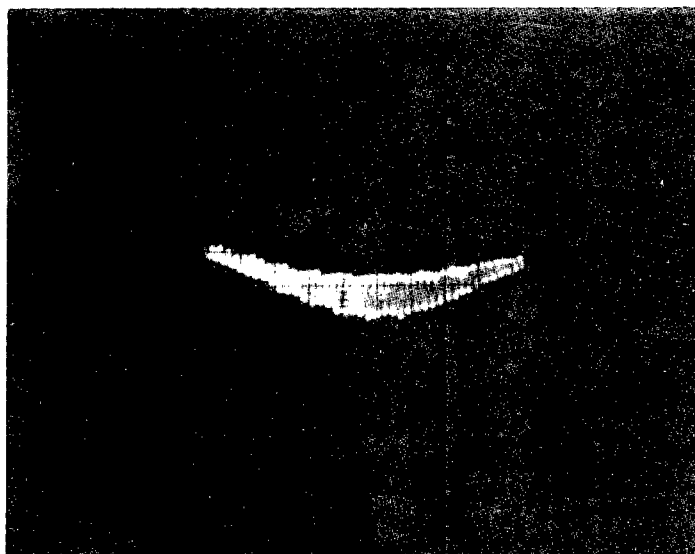
50 MICROSECONDS/CM

SWEEP SPEED

Figure 16. Integrated energy trace for NiTMD/DCE solution (1-cm cell).

OSCILLOSCOPE RESPONSE

10 MILLIVOLTS/CM



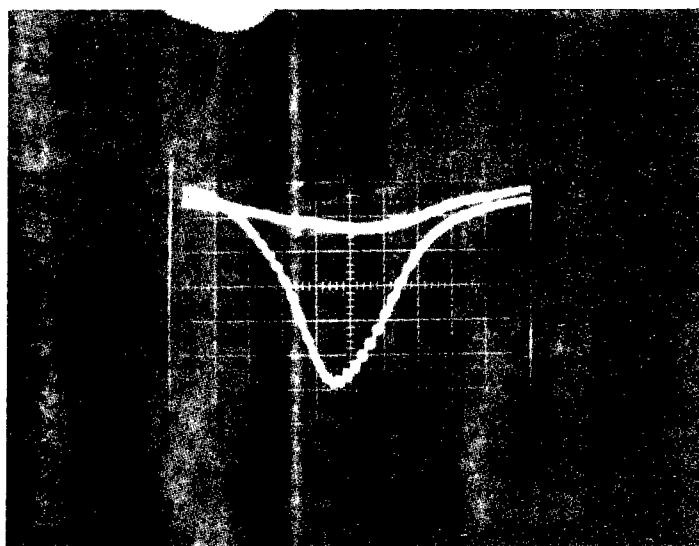
20 NANOSECONDS/CM

SWEEP SPEED

Figure 17. Power curve for NiTMD/MS solution (1-cm cell).

OSCILLOSCOPE RESPONSE

10 MILLIVOLTS/CM



20 NANOSECONDS/CM

SWEEP SPEED

Figure 18. Power curve for NiTMD/DCE solution (1-mm cell).

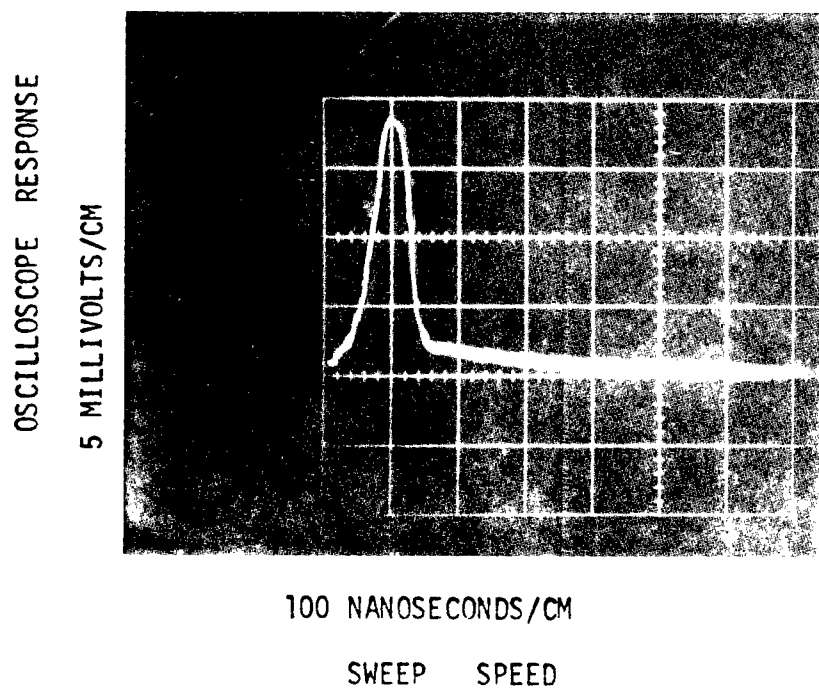


Figure 19. Power curve for NiTMD/DCE solution (1-cm cell).

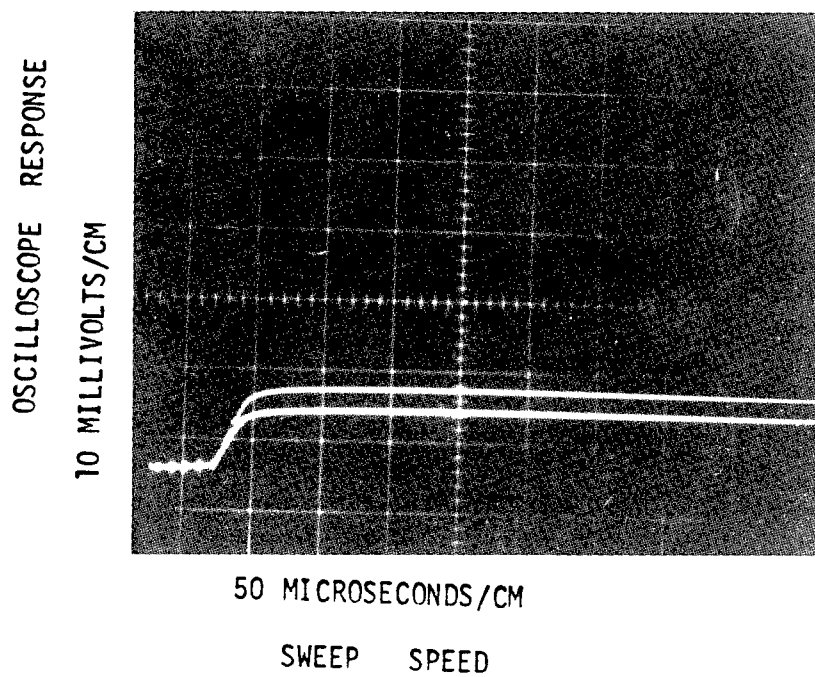


Figure 20. Integrated energy trace for PdTMD/DCE solution (5-mm cell).

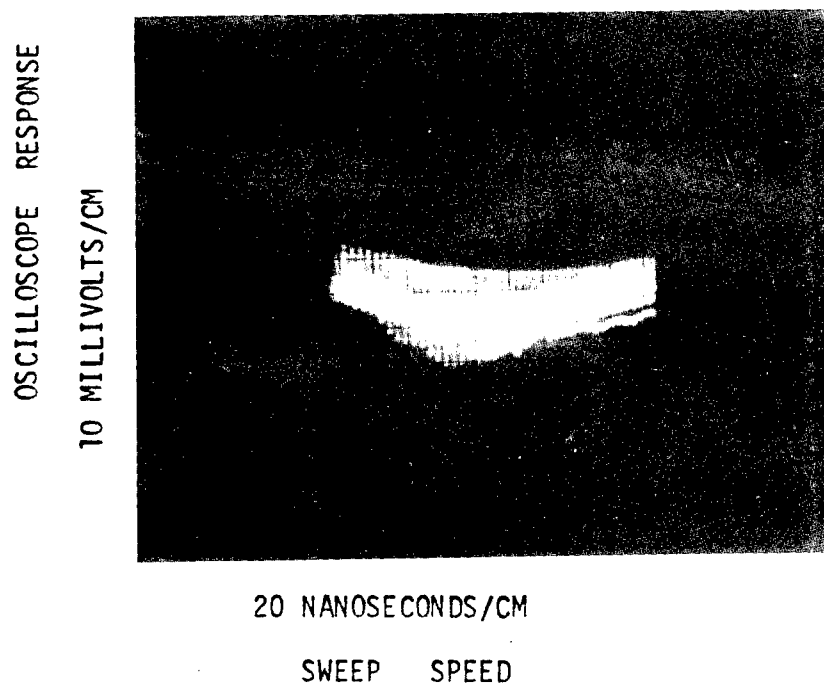


Figure 21. Power curve for PdTMD/MS solution (1-cm cell).

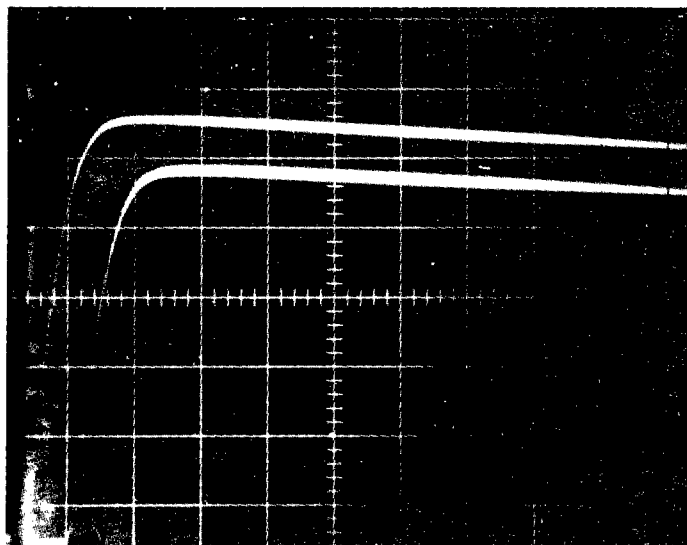
Pt-TMD (bis-(4,4'-dimethoxydithiobenzil)-platinum). This complex gave an absorption maximum of 860 nm in TCE solution and was more soluble in this solvent than the nickel and palladium complexes. The pink solution did not Q-switch the neodymium (1.06 μm) laser (Figures 22 and 23). The absorption maximum in DCE was at 865 nm, with ϵ_{max} being $4.22 \times 10^4 \text{ l-mol}^{-1}\text{-cm}^{-1}$.

Nd-ODD (bis-(4,4'-didecoxydithiobenzil)-nickel). Dissolved in CHCl_3 , this complex formed a dull green solution with absorption maximum at 935 nm. In CHCl_3 , ϵ_{max} has been reported as $3.39 \times 10^4 \text{ l-mol}^{-1}\text{-cm}^{-1}$.¹⁴ The DCE solution had an absorption maximum at 930 nm and an ϵ_{max} of $3.43 \times 10^4 \text{ l-mol}^{-1}\text{-cm}^{-1}$. The energy traces (Figures 24 and 25), show a high-energy Q-switched pulse, relatively stable to 10 p/s pulsing of the Nd:YAG laser. These traces and the power pulse of Figure 26 show that outputs comparable to Ni-DAD can be achieved, although longer path length cells were used.

¹⁴ C. Snyder, IBM Corp., private communication.

OSCILLOSCOPE RESPONSE

20 MILLIVOLTS/CM



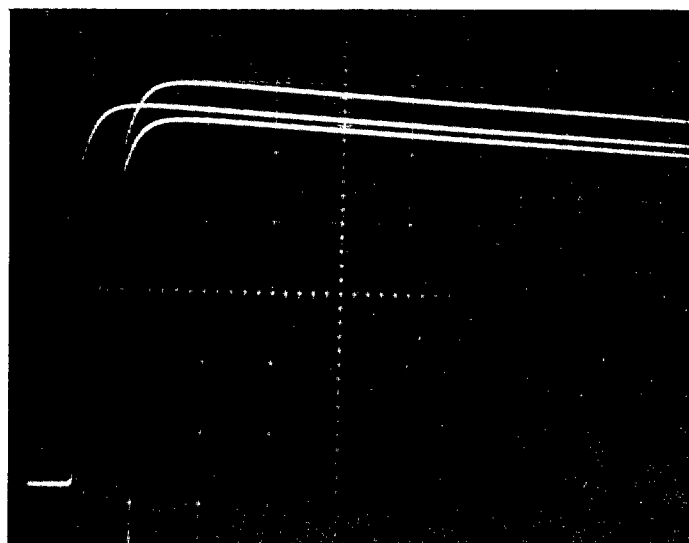
50 MICROSECONDS/CM

SWEEP SPEED

Figure 22. Integrated energy trace for PtTMD/TCE solution (1-cm cell).

OSCILLOSCOPE RESPONSE

50 MILLIVOLTS/CM



50 MICROSECONDS/CM

SWEEP SPEED

Figure 23. Integrated energy trace for PtTMD/DCE solution (2-cm cell).

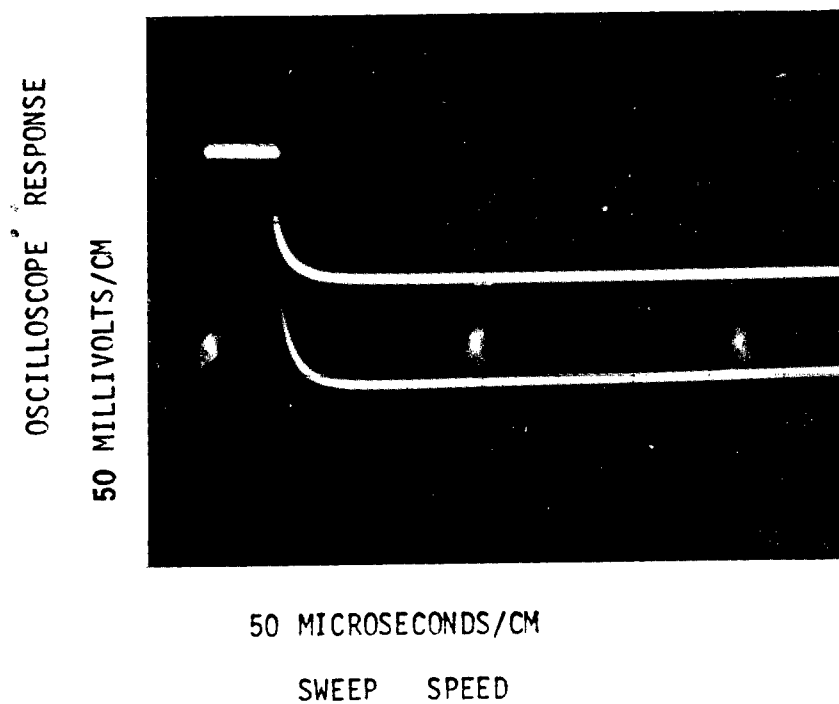


Figure 24. Integrated energy trace for NiODD/CHCl₃ solution (1-mm cell).

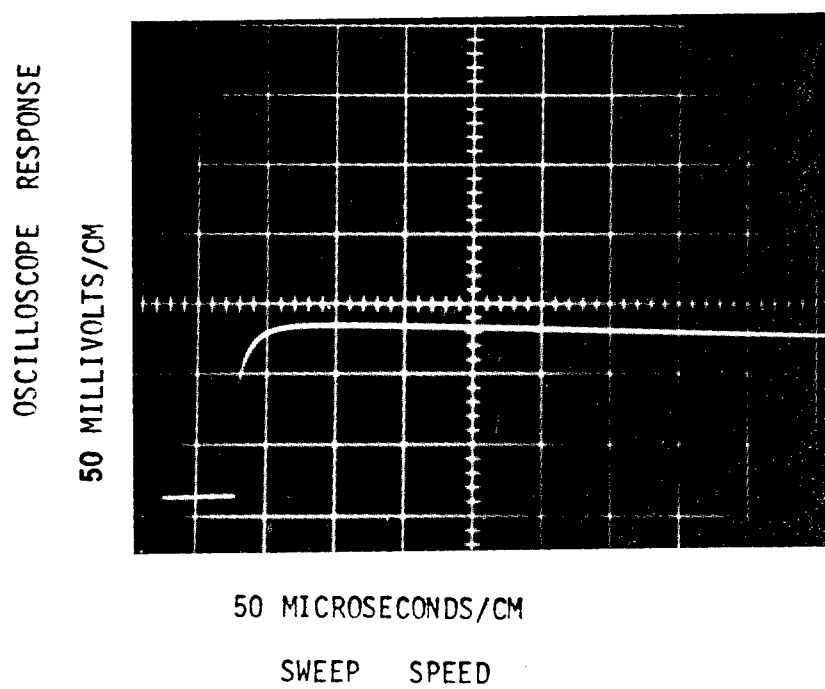


Figure 25. Integrated energy trace for NiODD/DCE solution (5-mm cell).

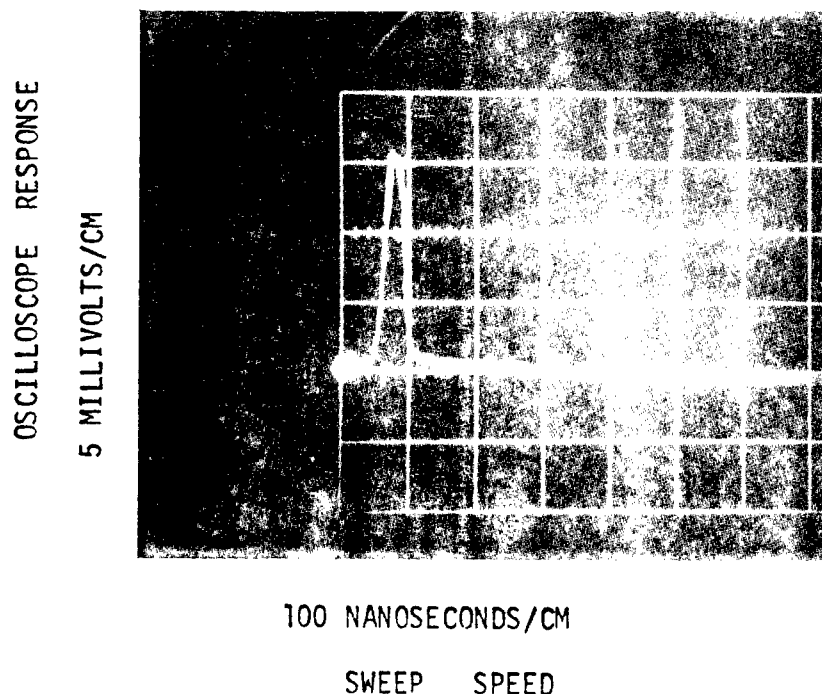


Figure 26. Power curve for NiODD/DCE solution (5-mm cell).

Ni-OCKD(bis-(4,4' dioxycarboxylic acid - dithiobenzil)-nickel, potassium salt). Water-soluble dyes present certain advantages in case of handling and would be particularly attractive if they functioned as a Q-switch for a near-infrared laser. Ni-OCKD is a water-soluble dye, with an absorption maximum at 920 nm and ϵ_{max} estimated to be $1.8 \times 10^4 \text{ l-mol}^{-1}\text{-cm}^{-1}$. Unfortunately, the dark green solution in either H_2O or D_2O did not Q-switch the Nd:YAG laser and only attenuated the laser emission.

Ni-OMeSD (bis-(4,4'-dioxycarboxylic acid - dithiobenzil)-nickel, methyl ester). This complex, the methyl ester from which the previous compound was derived, was evaluated in solvents CHCl_3 , MS, DCE, and Py. The absorption maxima of the green solutions range between 910 and 940 nm, ϵ_{max} being about $3 \times 10^4 \text{ l-mol}^{-1}\text{-cm}^{-1}$. None of the solutions Q-switched the neodymium laser.

Ni-OBED (bis-(4,4' dioxybutyric acid-dithiobenzil)-nickel, ethyl ester). The green solution of Ni-OBED in CHCl_3 had an absorption maximum at 925 nm; ϵ_{max} was reported to be $3.23 \times 10^4 \text{ l-mol}^{-1}\text{-cm}^{-1}$.¹⁴ Though the solution Q-switched the Nd:YAG laser (Figure 27), the output was variable.

¹⁴ C. Snyder, IBM Corp., private communication.

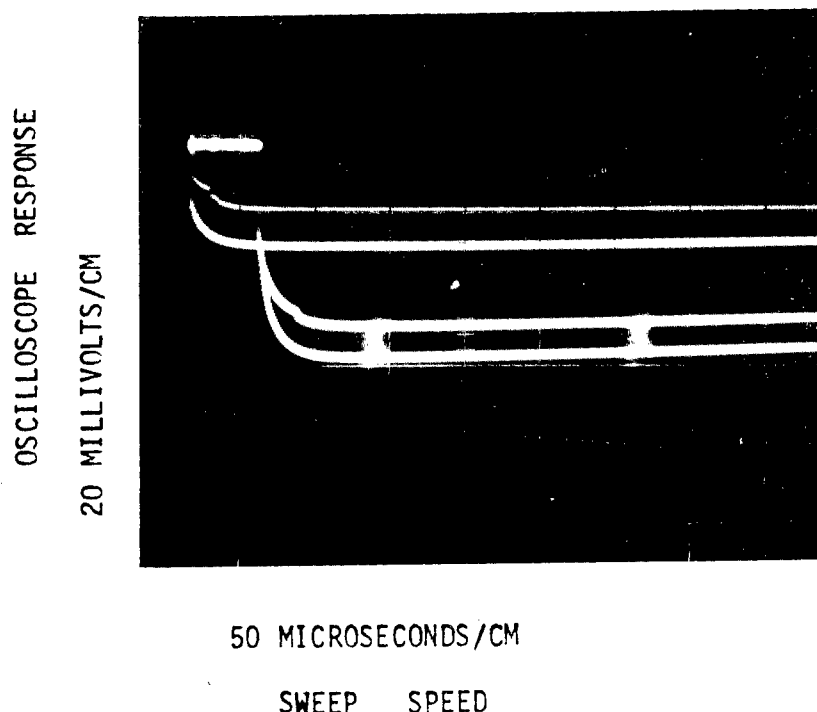


Figure 27. Integrated energy trace for NiOBED/ CHCl_3 (1-mm cell).

Ni-MJG (bis-(monojulolidinodithioglyoxal)-nickel). The CHCl_3 solution of Ni-MJG was pale yellow, with an absorption maximum at $1.55 \mu\text{m}$ and ϵ_{max} estimated to be $9.9 \times 10^3 \text{ l-mol}^{-1}\text{-cm}^{-1}$. The Nd:YAG laser was Q-switched by this solution (Figure 28).

Ni-DJG (bis(1,2-dijulolidinodithioglyoxal)-nickel). Ni-DJG formed a dark yellow-brown solution in DCE with an absorption maximum at $1.28 \mu\text{m}$ and ϵ_{max} estimated to be $2 \times 10^4 \text{ l-mol}^{-1}\text{-cm}^{-1}$. A maximum was found at $1.28 \mu\text{m}$ with $\epsilon_{\text{max}} = 1.9 \times 10^4 \text{ l-mol}^{-1}\text{-cm}^{-1}$ in DCE solution. The DCE solution Q-switched neither the neodymium laser nor the erbium laser.

Ni-TG (bis-(2-thienyldithioglyoxal)-nickel). In CHCl_3 , this complex exhibited maximum absorption at 908 nm with ϵ_{max} estimated at $2 \times 10^4 \text{ l-mol}^{-1}\text{-cm}^{-1}$. The green CHCl_3 solution Q-switched the Nd:YAG laser (Figure 29).

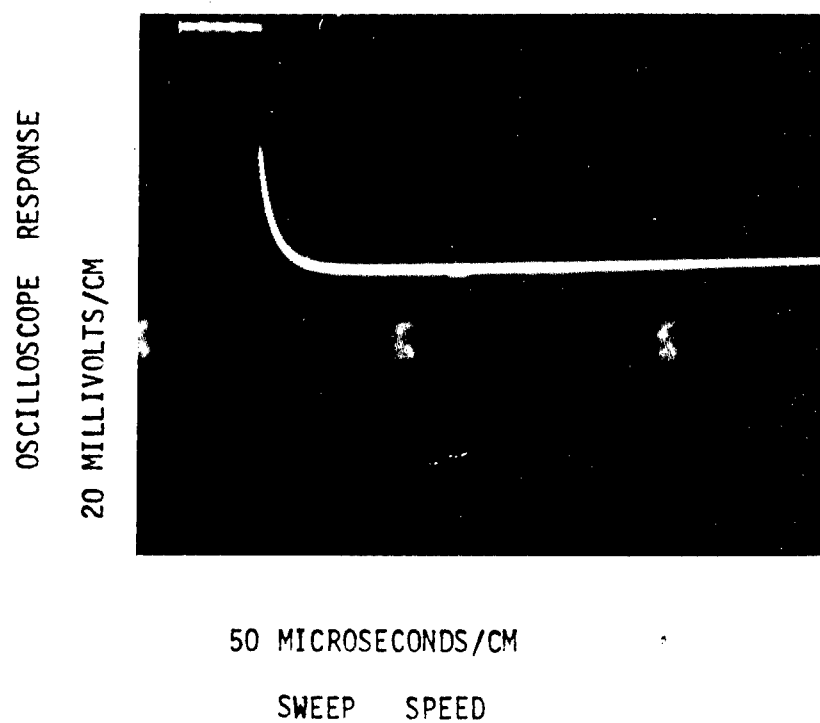


Figure 28. Integrated energy trace for NiMJG/CHCl₃ (1-cm cell).

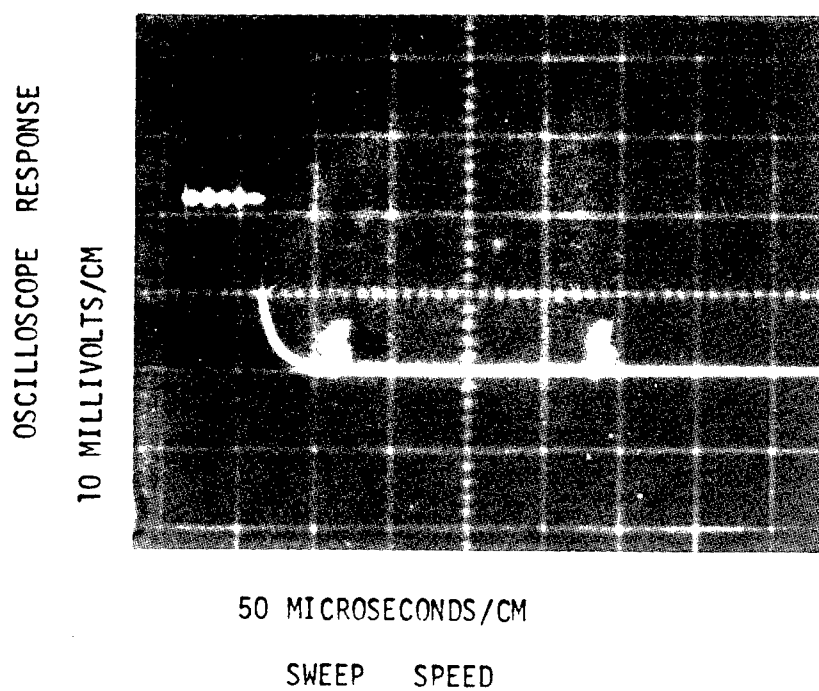


Figure 29. Integrated energy trace for NiTG/CHCl₃ (1-mm cell).

Ni-I (bis-(2,3-dithioindenedione)-nickel). A dark yellow-brown solution formed when this solution was dissolved in CHCl_3 , the absorption maximum being at 900 nm and ϵ_{max} about $1.1 \times 10^4 \text{ l-mol}^{-1}\text{-cm}^{-1}$. The solution gave two low-energy pulses with the Nd:YAG laser used. Single pulsing was not achieved.

Ni-DMI (bis-(5-dimethylamine-2,3-dithioindenedione)-nickel). This complex formed a dark brown solution in CHCl_3 . The absorption maximum was at $1.05 \mu\text{m}$, and ϵ_{max} was $5.6 \times 10^3 \text{ l-mol}^{-1}\text{-cm}^{-1}$. The solution Q-switched the Nd:YAG laser, but its performance was somewhat variable (Figures 30 and 31).

Ni-DTAQ (bis-(dithioacenaphthenequinone)-nickel). Ni-DTAQ was examined in DMF solution, forming a dark yellow solution. Its maximum absorption was at $1.14 \mu\text{m}$; ϵ_{max} was not determined due to poor solubility. No Q-switching of the Nd:YAG laser was observed.

Ni-DTPQ (bis-(dithiophenanthrenequinone)). A light yellow solution formed when Ni-DTPQ was dissolved in DMF. The absorption maximum was at $1.01 \mu\text{m}$, but poor solubility deterred a determination for ϵ . No evidence for Q-switching the Nd:YAG laser was found.

2. KBr as a Host Medium. Liquid solvents, as used in the Q-switch evaluations described above, are convenient for laboratory use. But as the dithiene molecular structures become more complex, the compound can be expected to be less soluble in the liquids available that are transparent in the near infrared. A solid host is preferable for field use, thus further reducing the desirability of working with liquid media. In infrared absorption studies, the compound of interest is often dispersed in a potassium bromide matrix in pellet or wafer form. KBr pellet techniques may provide a resolution to the Q-switch host material in the near infrared as well.

Preliminary studies to determine the feasibility of using KBr as a Q-switch host material were carried out within the limitations of available resources. KBr was reputed to be sufficiently transparent in the near infrared.¹⁵ Absorption measurements made on a 5-mm thick optical quality KBr disc (Perkin-Elmer Corp. No. 027-1202) indicated that a 1-mm thick wafer, comparatively clear, would have an absorbance of only about 0.02 absorbance units between $0.8 \mu\text{m}$ and $2.15 \mu\text{m}$. The Q-switch solutions in this study usually had absorbances in the 0.35 unit range. A Wilks Mini-Press was used to prepare Ni-DAD/KBr pellets from Harshaw infrared grade potassium bromide. Uniform dispersion of Ni-DAD powder in KBr was accomplished with a Perkin-Elmer Mini Vibrator. Translucent 1-mm thick pellets were formed, colorless for KBr alone and greenish when Ni-DAD was incorporated. The KBr + Ni-DAD pellet gave an optical density (absorbance) reading of 0.36 at $1.06 \mu\text{m}$, though the absorption maximum was shifted to $1.15 \mu\text{m}$ with an optical density of 0.4.

¹⁵ G. Harrison, R. C. Lord, and J. R. Loofbrow, *Practical Spectroscopy*, Prentice-Hall, Inc., p. 52, (1946).

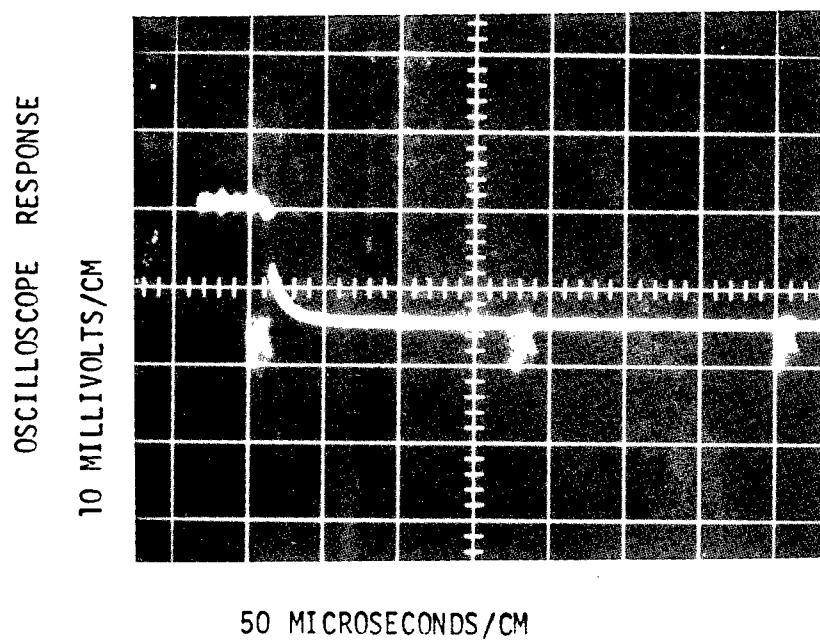


Figure 30. Integrated energy trace for NiDMI/CHC1₃ (1-mm cell).

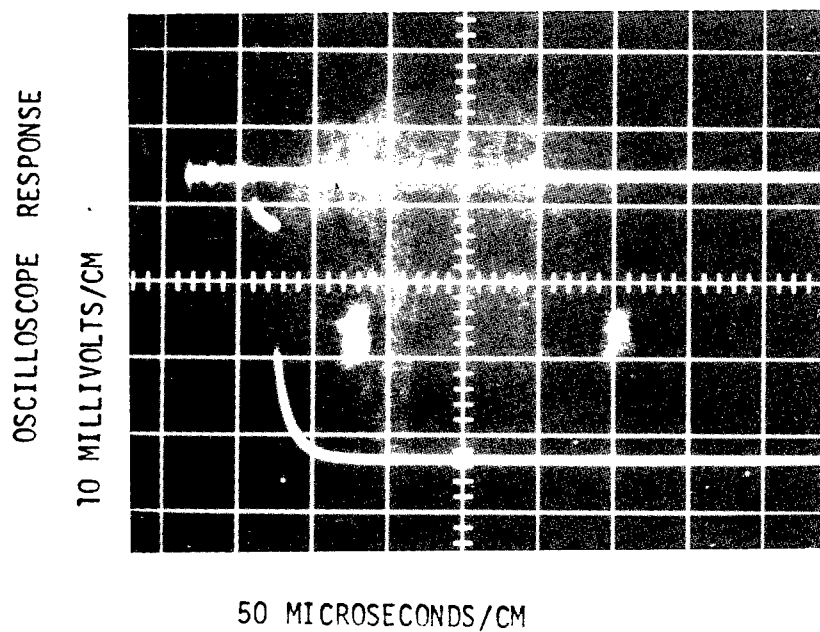


Figure 31. Integrated energy trace for NiDMI/CHC1₃ (1-mm cell).

Both the KBr blank pellet and the KBr + Ni-DAD pellet held off the Nd 1.06 μm laser emission. The laser was the same laser used in paragraph 1, above. No such transmission problem was encountered when infrared optical absorption cells, or even ordinary microscope slides, were used. We attribute the difficulty cited here with KBr pellets to be a consequence of the limitations of the KBr pressing technique used. Until clear pellets are produced using more refined techniques and tested with appropriate lasers, no final conclusions can be made concerning KBr as a Q-switch host medium.

3. Optical Saturation Studies. Saturable absorbers treated in this report are principally those with absorption maxima around 1 μm . Testing with a neodymium laser was adequate for determining Q-switch performance for most of these compounds. New compounds will be created as the result of molecular engineering efforts to design dyes with absorption maxima extending toward 2 μm , however. A serious limitation to the evaluation of the success of the molecularly engineered Q-switch candidates can be expected to be caused by the lack of a laser with emission corresponding to the absorption maximum of the candidate compound. A tunable near-infrared laser will be needed. Dye lasers are available, emitting tunable radiation in the 1 μm to 2 μm range of interest to us. The near-infrared emission is achieved with an optical parametric oscillator installed externally to the laser cavity so that the procedure in paragraph 1 of this report, in which the passive Q-switch cell is mounted inside the laser cavity, would be useless. Even if 1 μm to 2 μm emitting laser dyes were available, the probability is that we would see mode-locking at best and not the desired single giant pulse. Only one case of single pulsing a dye laser with a passive Q-switch has been reported, in fact.¹⁶ We require a testing method in which the performance of a saturable absorber dye can be evaluated when it is placed externally to a tunable dye laser cavity.

One can expect that the transmission of a dye solution will vary as the power density of the incident light changes. At a sufficiently high power density, a good saturable absorber dye would be completely bleached, or "open." Optical saturation studies have been reported on saturable absorber dyes used with ruby lasers, on robust laser absorber dyes (for eye protection devices) irradiated with a neodymium laser, and on Ni-DAD solutions.^{17 18 19 20} We initiated studies here to determine the feasibility of using optical saturation techniques on new dithiene dyes, using the neodymium laser of paragraph 1. Extension of the technique to the use of an actively Q-switched, tunable, near-infrared dye laser was not begun at the time this report was written.

¹⁶ L. W. Braverman, *Appl. Phys. Ltrs.*, 27(11), 602 (1975).

¹⁷ M. L. Spaeth and W. R. Sooy, *J. Chem. Phys.* 48(5), 2315 (1968).

¹⁸ W. R. Sooy, et al., "Saturable Dye Optical Switch Investigation," US Army Electronics Command Technical Report ECOM-01237-F, Ft. Monmouth, NJ (December 1966).

¹⁹ J. D. Margerum, et al., "Studies on Passive Q-Switch Materials for Lasers," US Air Force Materials Laboratory Technical Report AFML-TR-73-106, AD-778 066, Defense Documentation Center, Alexandria, VA (June 1973).

²⁰ M. W. Windsor, "The Effects of Picosecond Laser Pulses on Dyes Employed for Laser Countermeasures," Final Report, US Army Frankford Arsenal Contract DAAA27-5-73-CO-208 (September 1978).

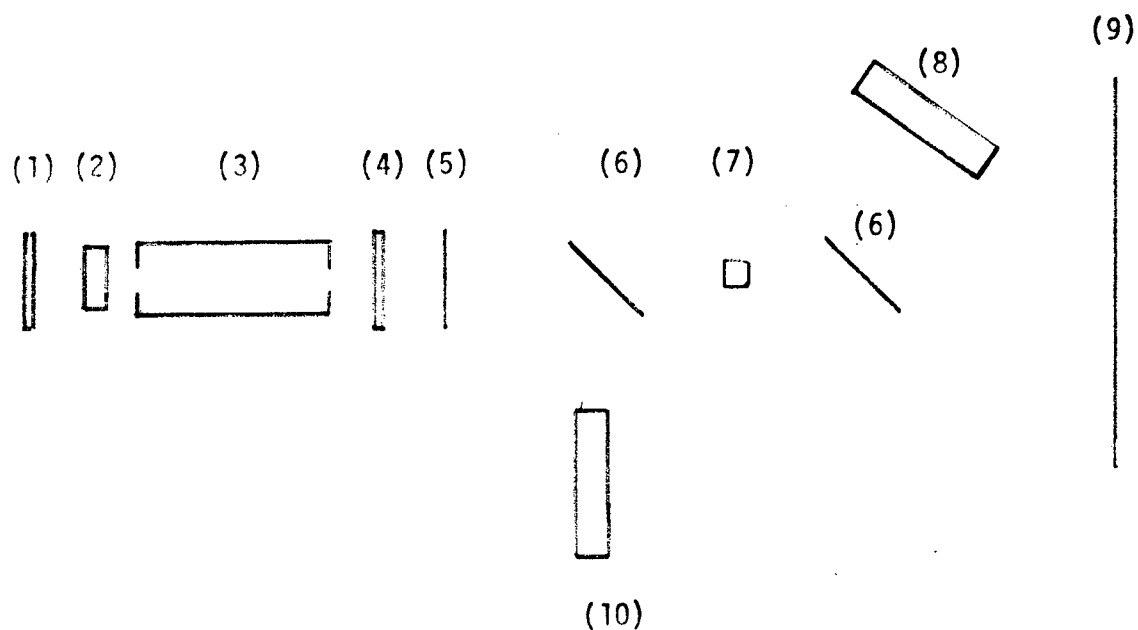
The experimental apparatus used is outlined in Figure 32. A Nd:YAG laser (paragraph 1) was actively Q-switched with a KD*P Pockel Cell. The 1.06 emission was attenuated with Wratten neutral density filters (0.0, 0.2, 0.3, 0.2+0.2, and 0.3+0.3 values) between glass microscope slides. Enough variation in power density was obtained in this way to indicate trends in performance of the dithienes. A wider range of values would be obtained with a more powerful laser and more sensitive detectors. Less scatter would have been attained, perhaps, had variable Glan attenuating prisms been used instead of neutral density filters. A beam splitter divided the 20-ns laser pulse as shown in Figure 32. Two SD100 detectors were used, monitored on a Tektronix 485 oscilloscope. Calibration of the oscilloscope response for each detector was accomplished with a TRG 101 Thermopile. Readings for detector No. 1 provided I_0 values, and I values were obtained from detector No. 2. Transmission values as percentages were calculated from $(I/I_0) \times 100$.

Optical saturation curves are presented in Figures 33 through 50. Low-level transmission values at 1.06 μm were calculated from spectrophotometric absorption measurements made on each test cell. These low-level transmissions are shown as dashed horizontal lines on each curve. Except where indicated otherwise, these are optical transmission values at 1.06 μm . The effective transmission level, especially for dyes with absorption maxima displaced up to $\pm 0.1 \mu\text{m}$ from the laser wavelength, may reflect transmission values at the maximum of absorption. The absorption band observed for dyes and other organic molecules corresponds to at least one electronic transition and its associated transitions between vibrational and rotational levels. Invoking the steady state assumption, population of nearby empty levels may occur. Multiphoton transitions are possible, also. A two electron transition has been postulated for the relaxation process in Ni-DAD.⁸ The effective transmission for a dye pumped by intense Nd laser emission (line width ca. 50 Å in some commercial models) therefore, conceivably may be somewhat less than that obtained with a spectrophotometric scan (3 Å resolving power). A Nd emission at 0.91 μm has been reported, but because of the selectivity of the 1.06 μm mirrors used in our system, such emission is believed to be negligible here. Only the 1.06 μm radiation is believed to generate absorption processes in the dye. Figures 33 and 34 present the data for two commercially available 1.06 μm Q-switches of the cyanine type, Eastman Kodak No. 9740 (in Eastman reagent grade chlorobenzene) and No. 9860 (in DCE). Figure 35 is a similar curve for bisfulvalene dicobalt-PF₆ in benzonitrile solution.²¹ This compound was a good absorber at 1.06 μm ($\lambda_{\text{max}} = 0.94 \mu\text{m}$, $\epsilon \sim 4.6 \times 10^3 \text{ liter-mole}^{-1}\text{-cm}^{-1}$), but did not Q-switch the Nd:YAG laser of paragraph 1. Figures 33 and 34 indicate the "opening" or rapid rise in transmission found for saturable absorbers, while little change in transmission is found in Figure 35 for a non-Q-switching absorber. Figures 36 through 50 are the optical saturation curves for the dithienes. Table 1 compares the Q-switch results of paragraph 1 and the opening data found here. Consistent agreement at 1.06 μm was found between definite Q-switching performance and "opening" in the optical saturation curves. The agreement would support the use of optical saturation curves, determined at the absorption maximum of any new dithiene candidate dye, to indicate Q-switching potentiality.

⁸ D. Magde, B. A. Bushaw, and M. W. Windsor, *Chem. Phys. Lett.* 28(2), 263 (1974).

⁹ K. H. Drexhage and U. T. Muller-Westerhoff, *IEEE J. of QE*, QE-8(9), 759 (1972).

²¹ Compound supplied by U. T. Mueller-Westerhoff, IBM Research Laboratory.



- LEGEND: (1) 100% reflecting mirror
 (2) KD*P Pockel cell
 (3) Neodymium-YAG laser
 (4) 85% reflecting mirror
 (5) Neutral density filter
 (6) Beam splitter
 (7) Dye cell
 (8) Detector #2
 (9) White reflector
 (10) Detector #1

Figure 32. Experimental configuration for optical saturation studies.

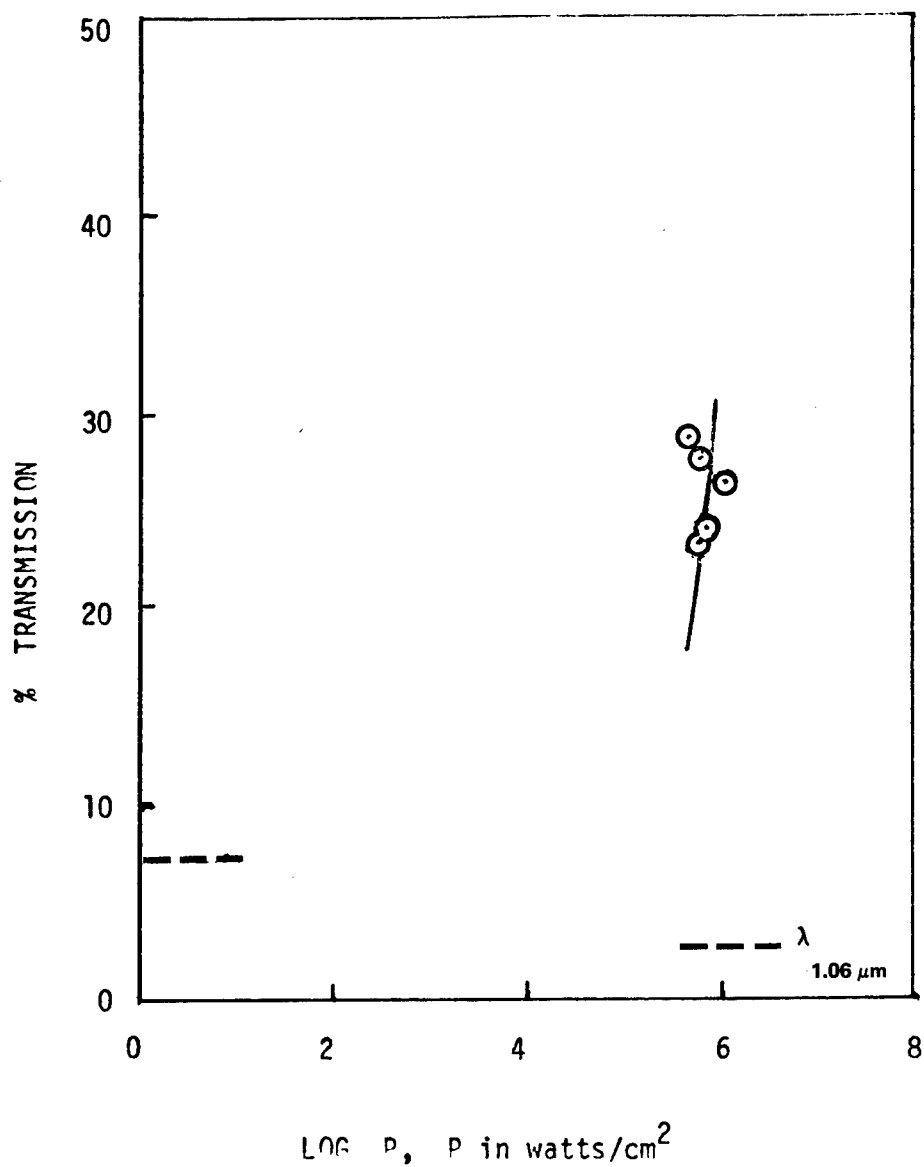


Figure 33. Optical saturation of EK No. 9740/chlorobenzene solution.

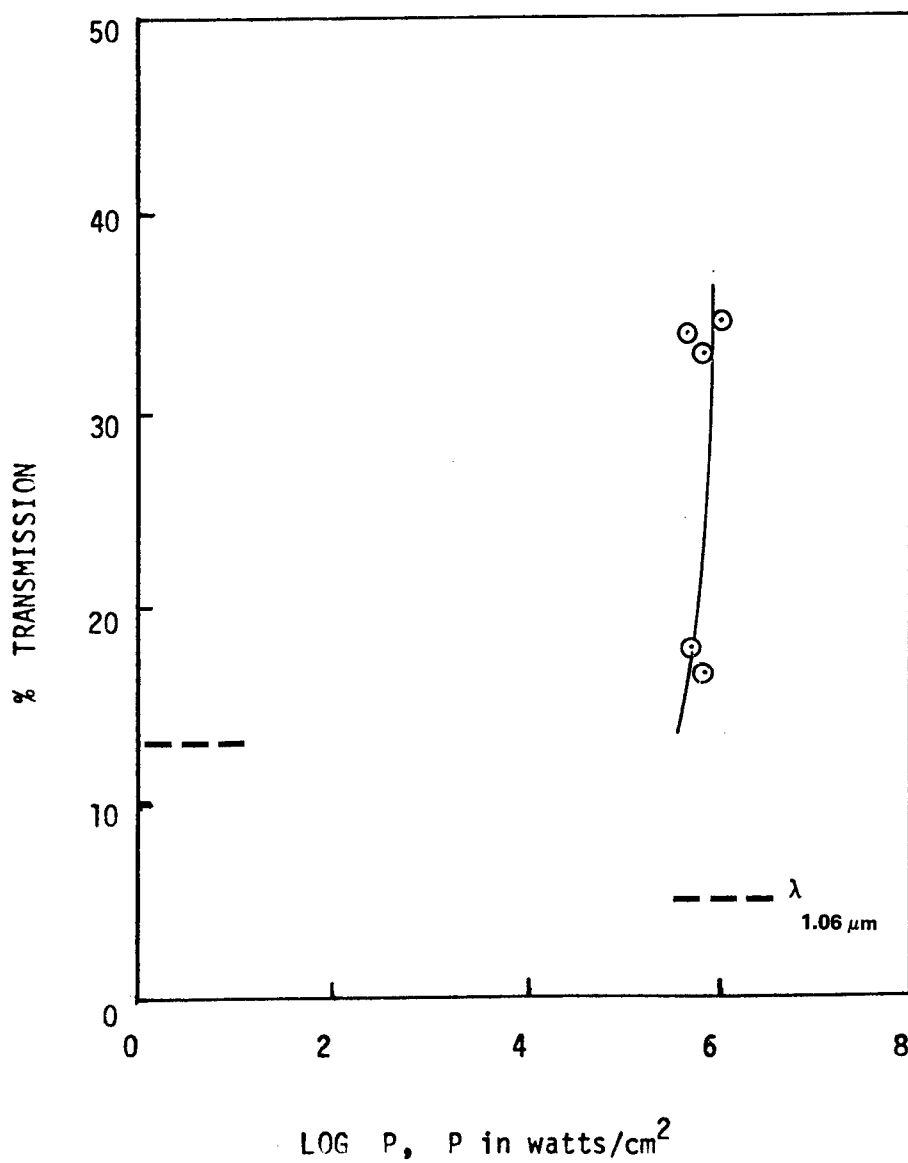


Figure 34. Optical saturation of EK No. 9860/DCE solution.

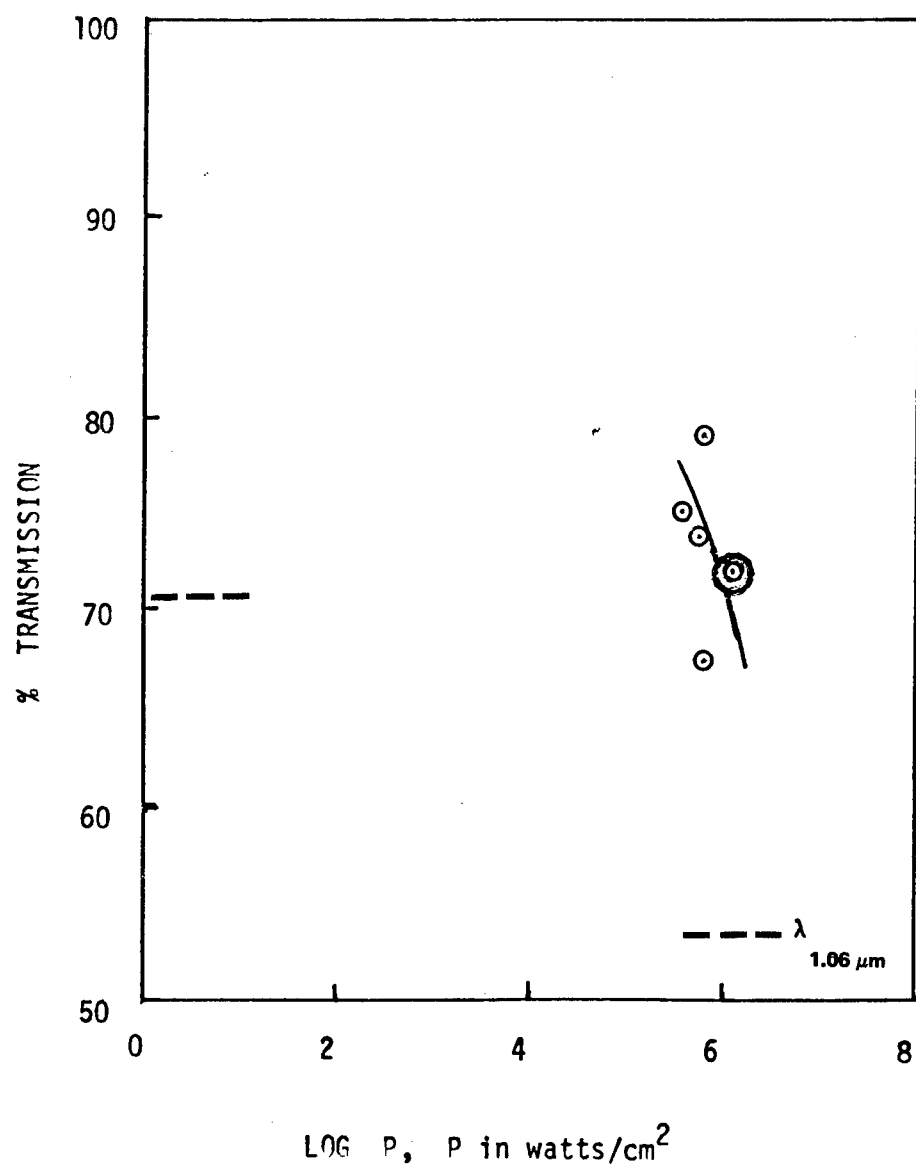


Figure 35. Optical saturation of BFCO₂ PF₆/Benzonitrile solution.

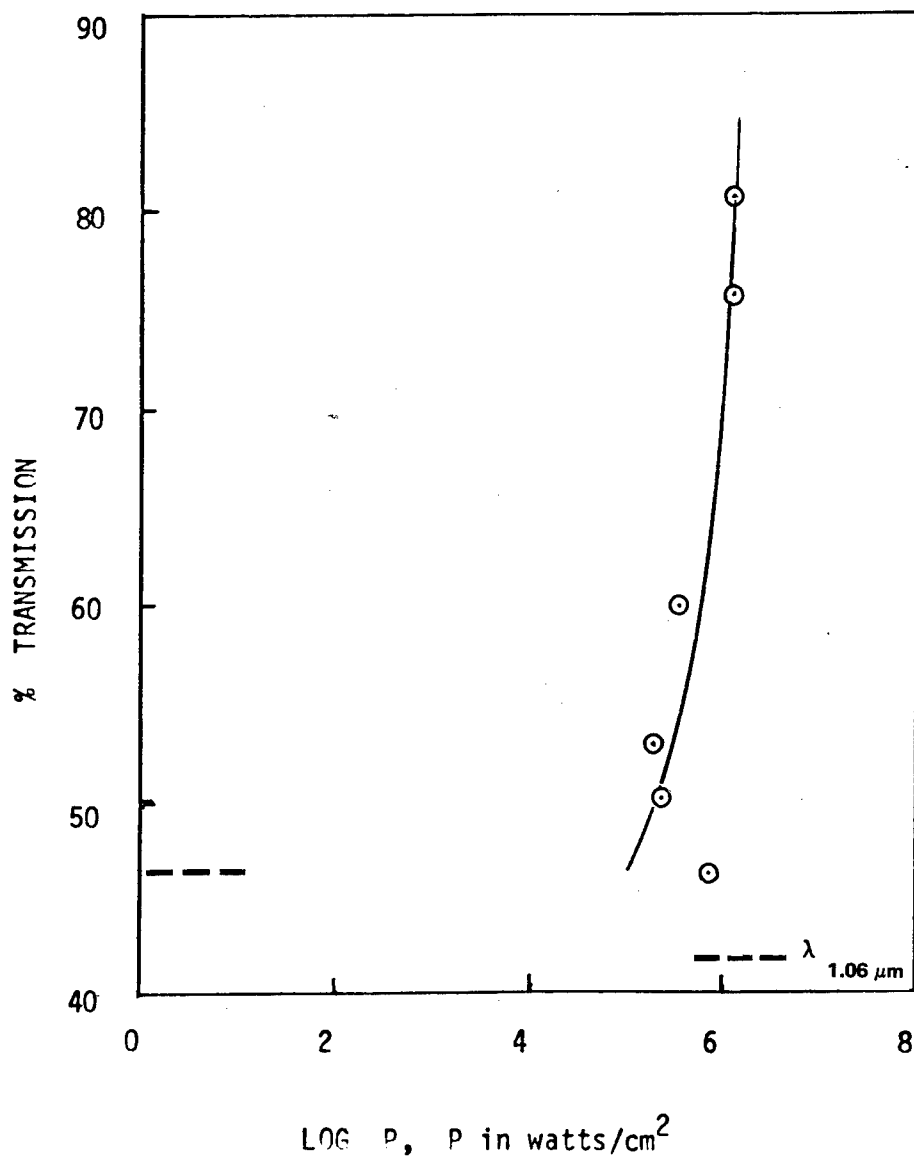
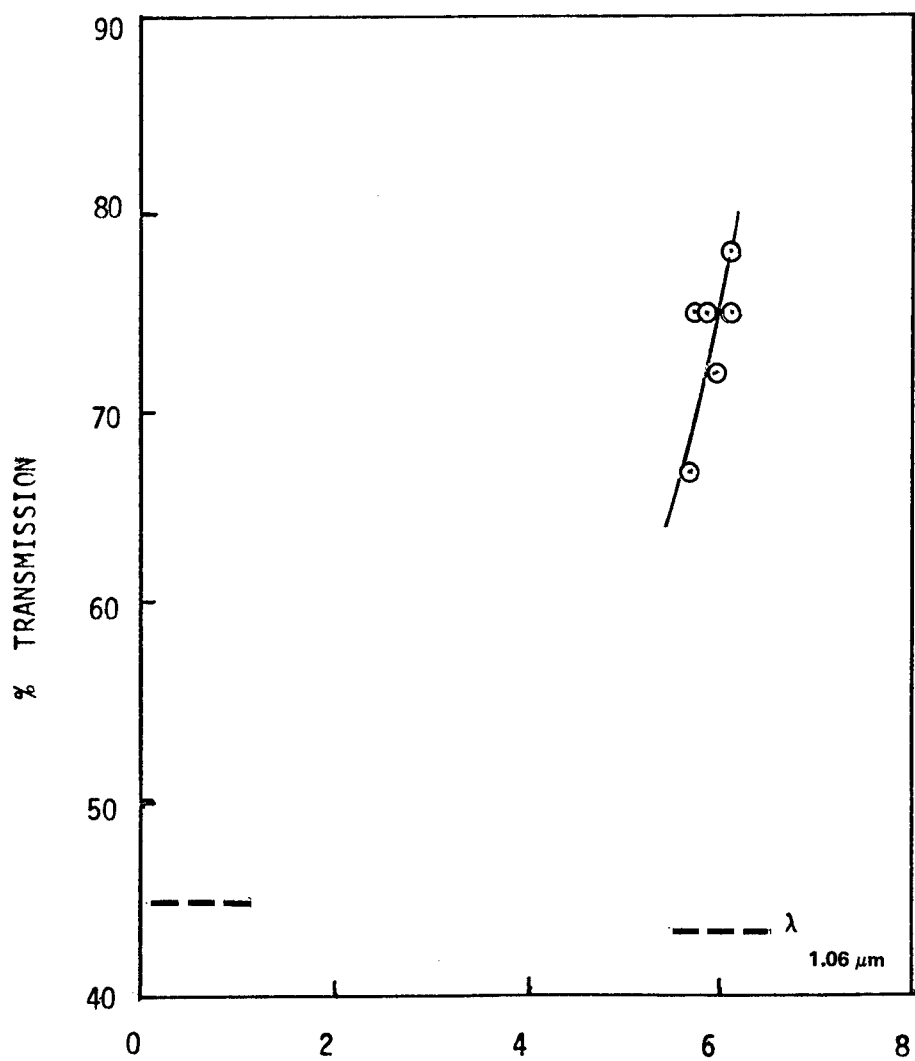


Figure 36. Optical saturation of Ni-DAD/DCE solution.



LOG P, P in watts/cm²
Figure 37. Optical saturation of NiTG/CHCl₃ solution.

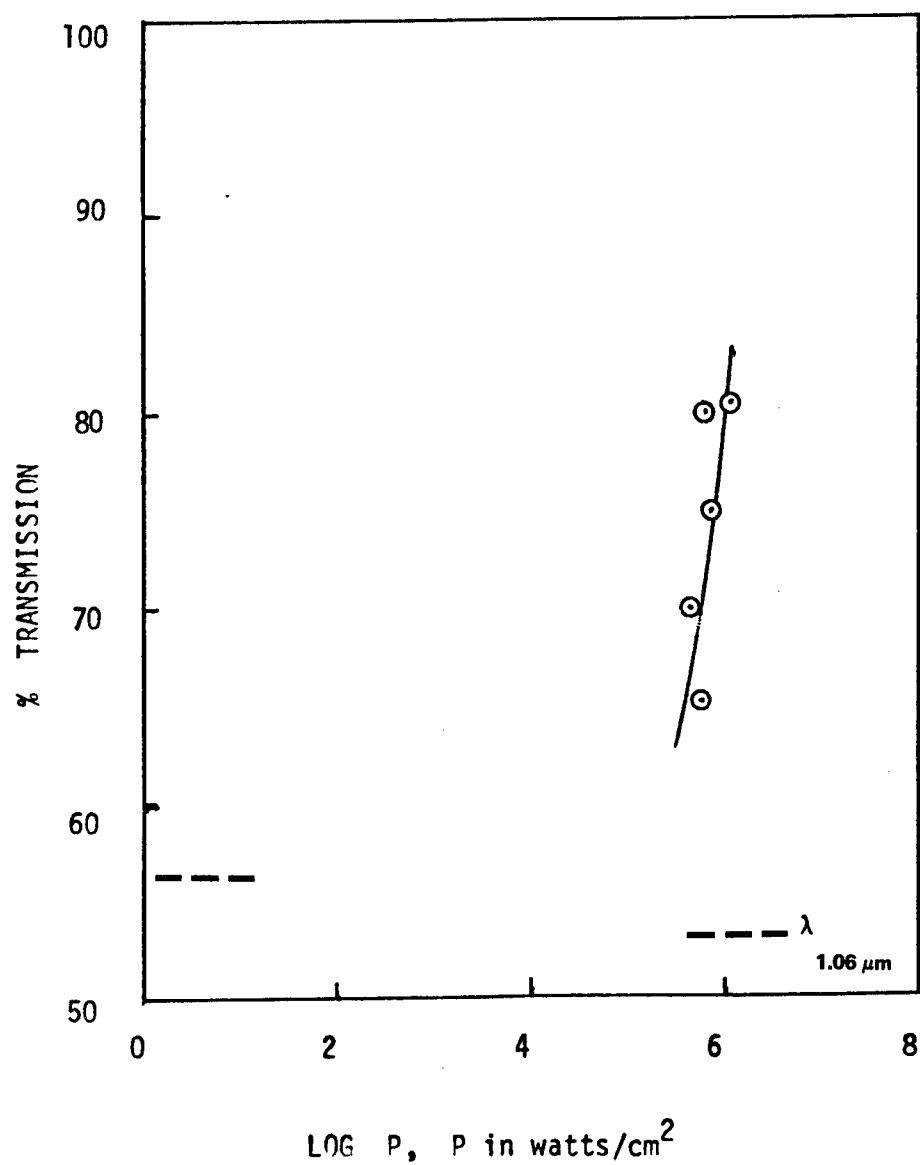


Figure 38. Optical saturation of Nil/CHCl₃ solution.

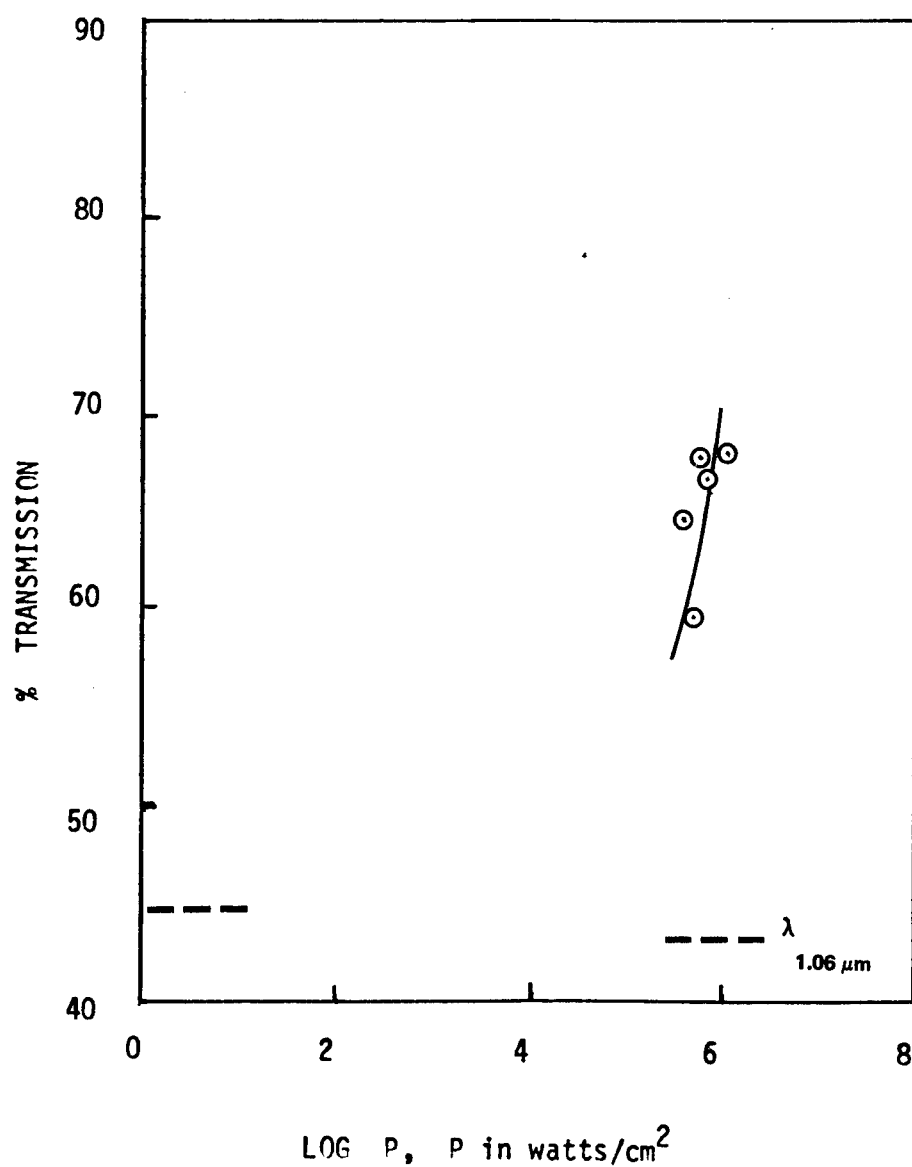


Figure 39. Optical saturation of NiODD/CHCl₃ solution.

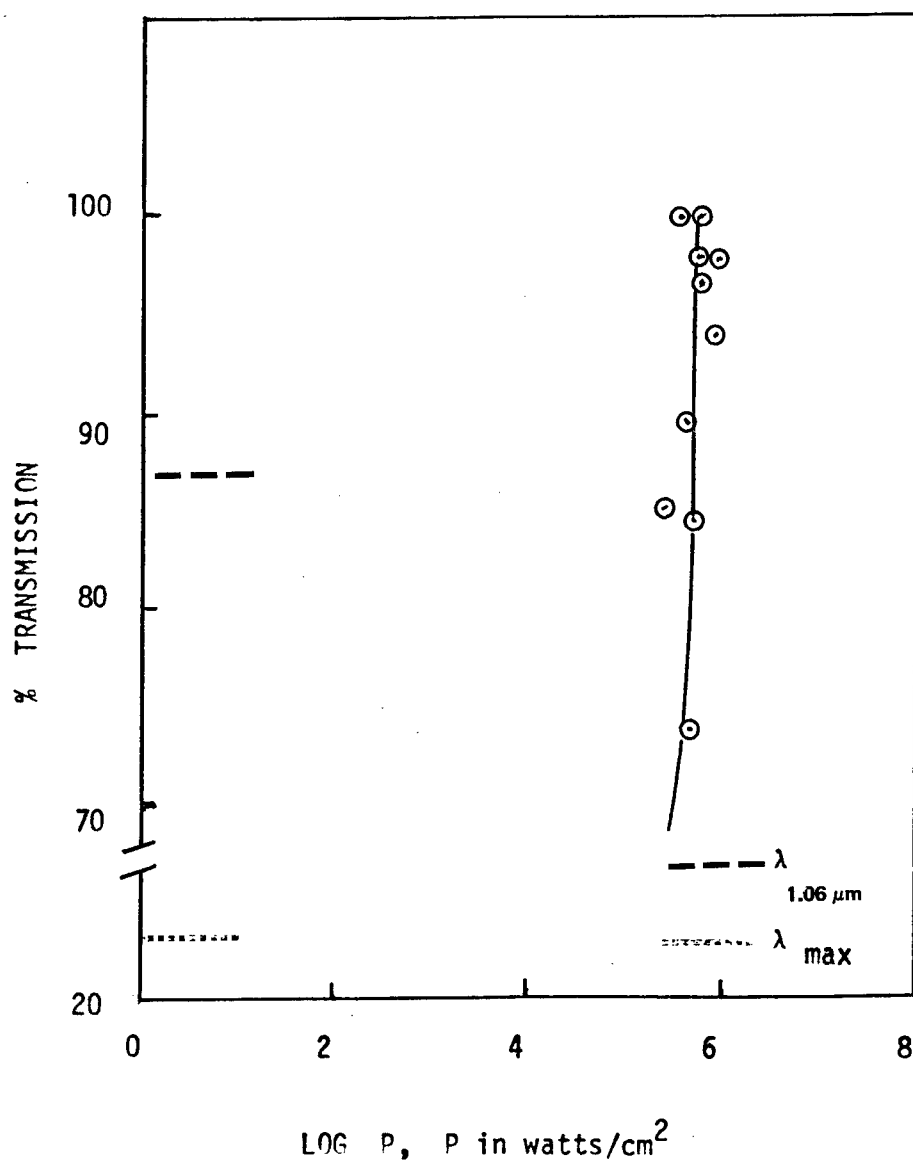


Figure 40. Optical saturation of NiMJG/CHCl₃ solution.

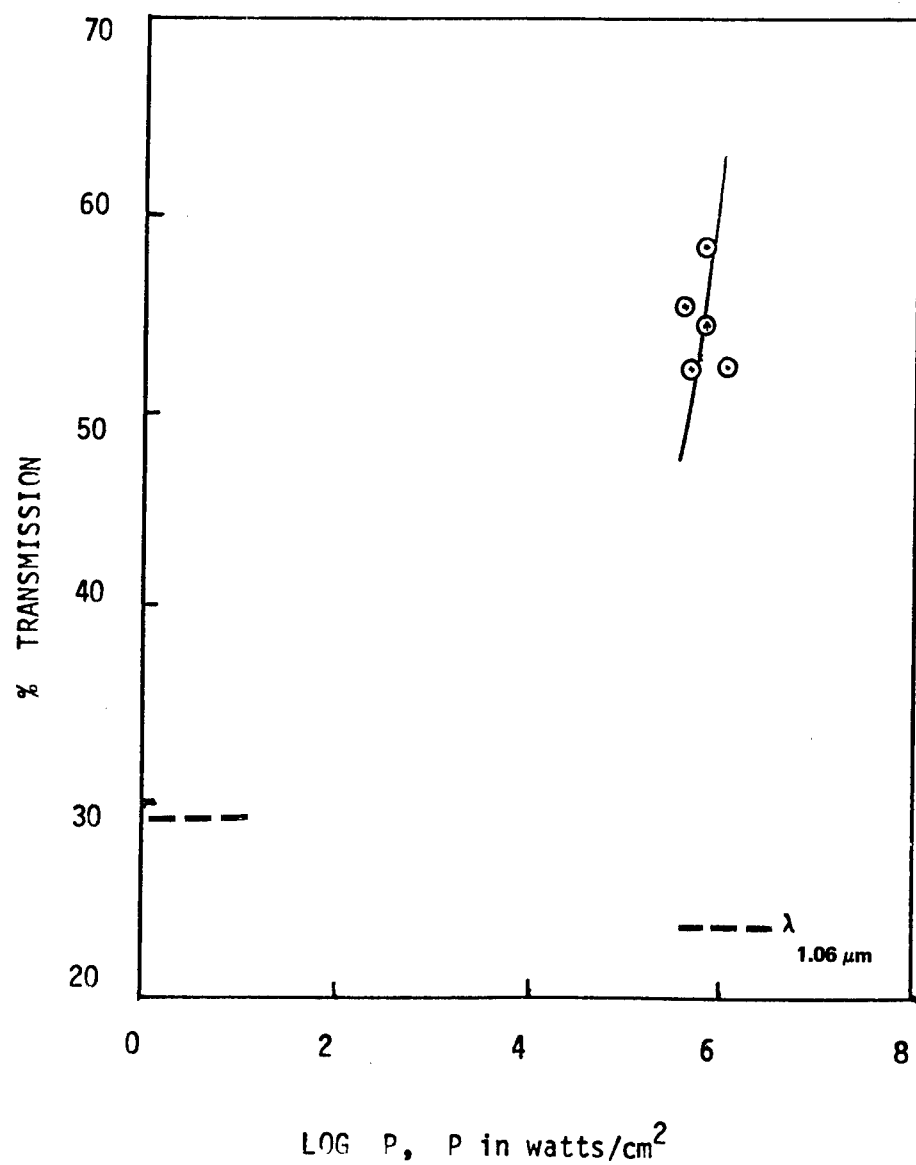


Figure 41. Optical saturation of NiOBED/CHCl₃ solution.

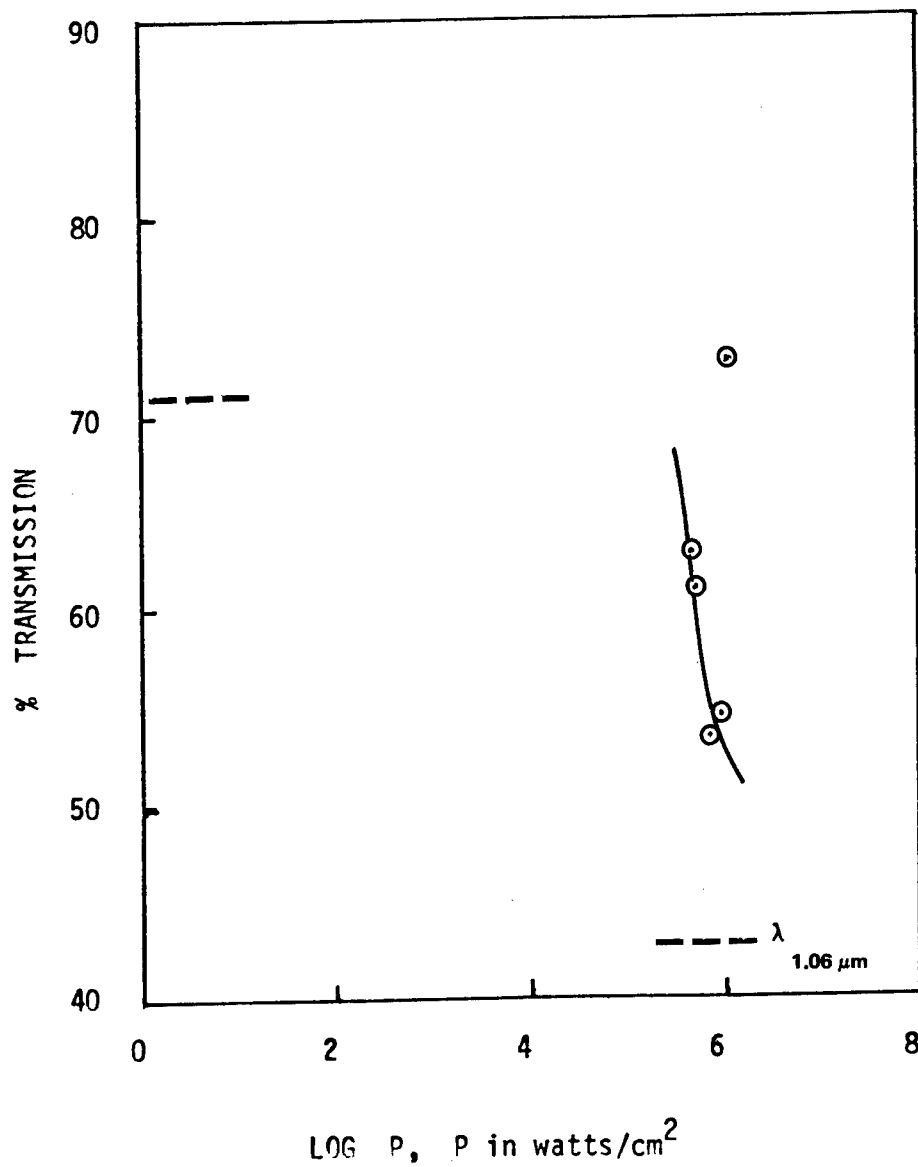


Figure 42. Optical saturation of NiOMeS/DCE solution.

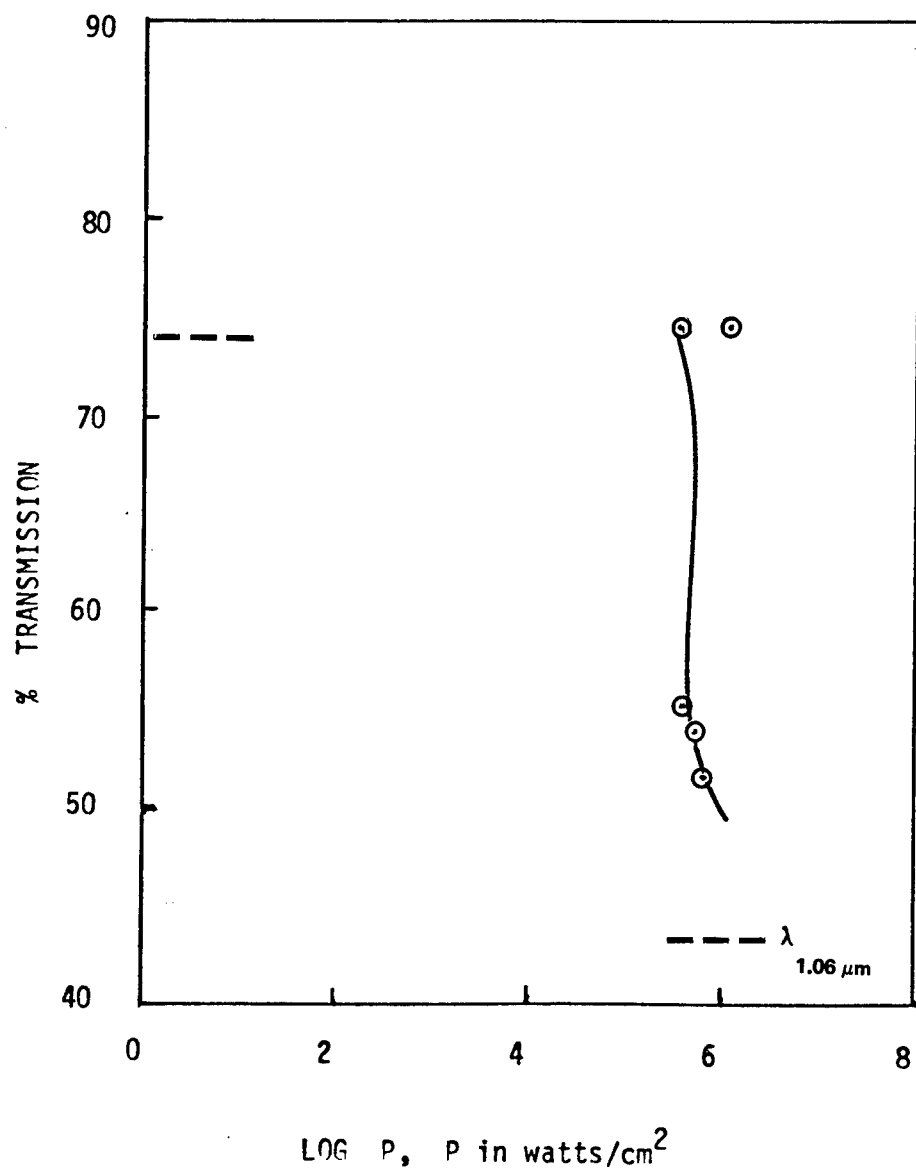


Figure 43. Optical saturation of NiDMI/CHCl₃ solution.

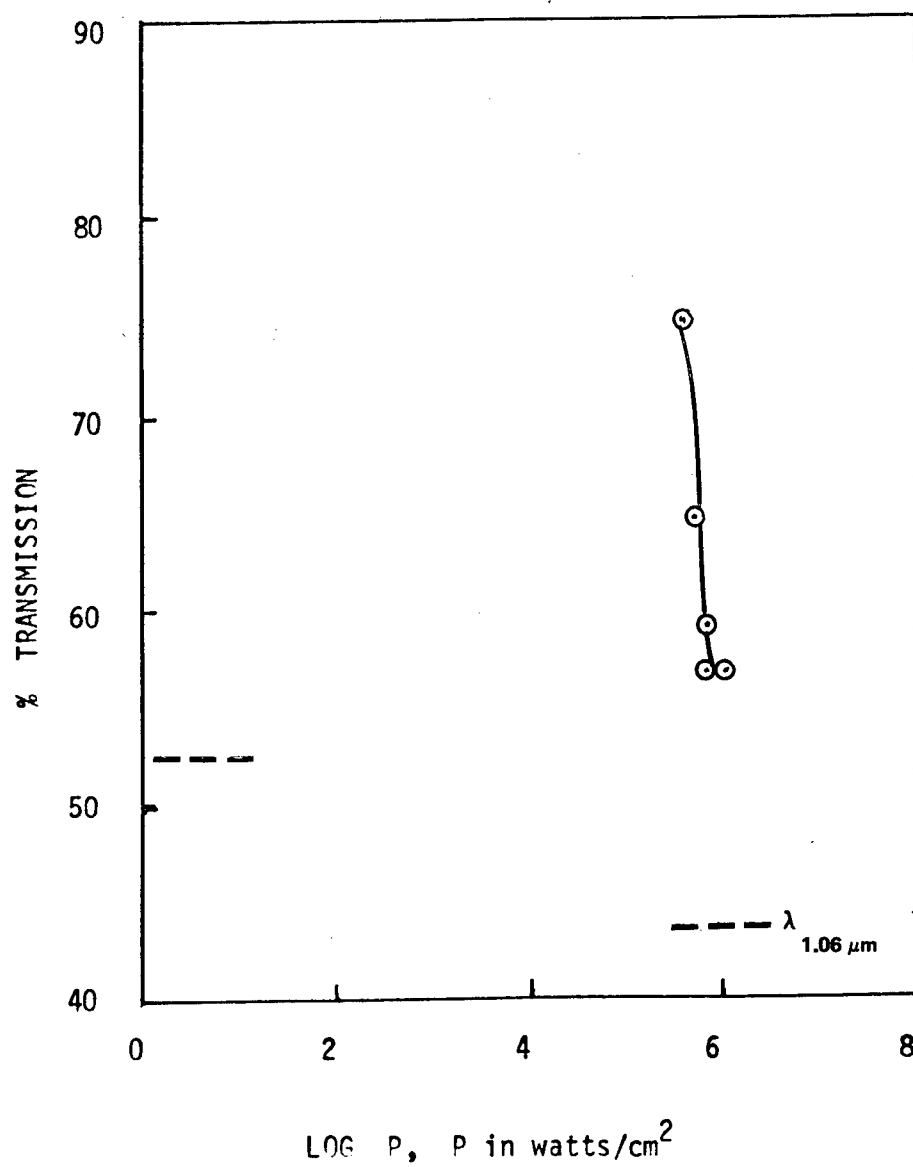


Figure 44. Optical saturation of NiD/CHCl₃ solution.

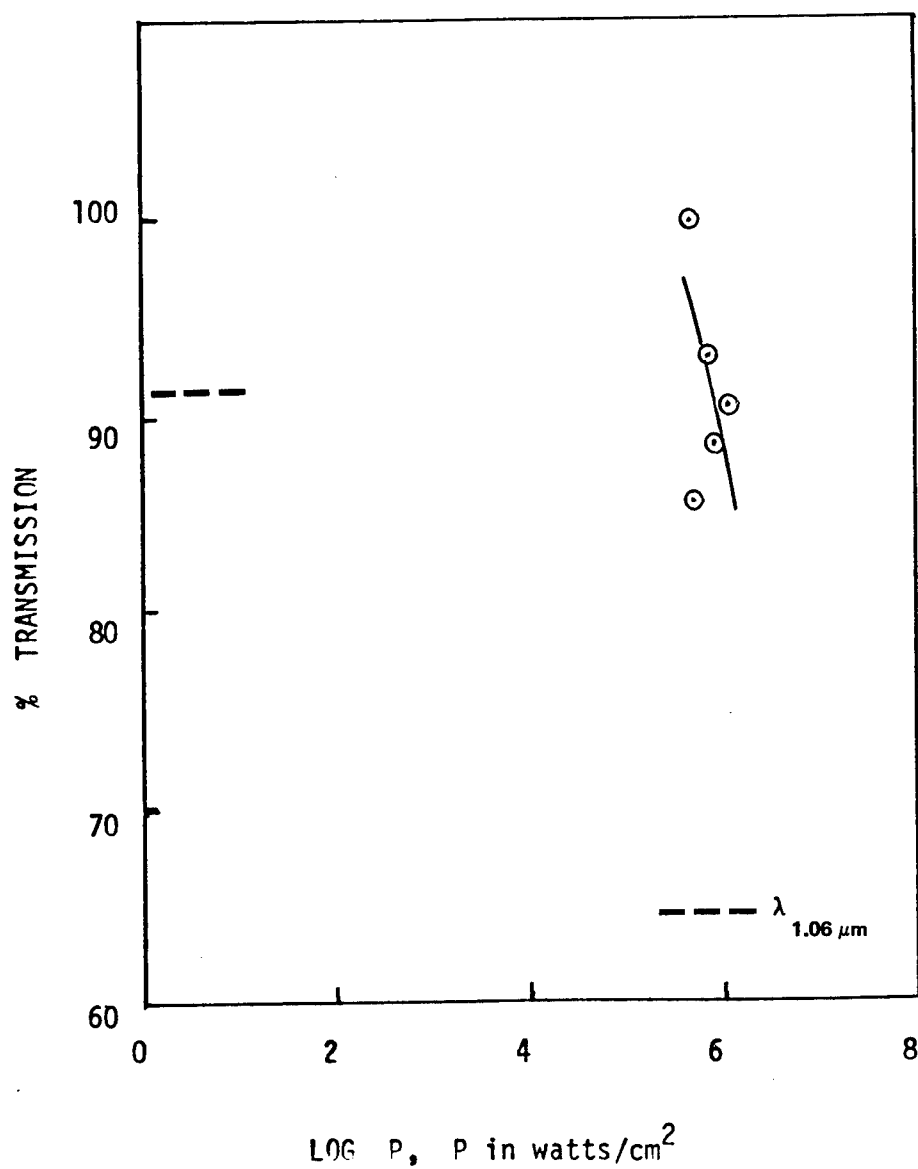


Figure 45. Optical saturation of NiDTPQ/DMF solution.

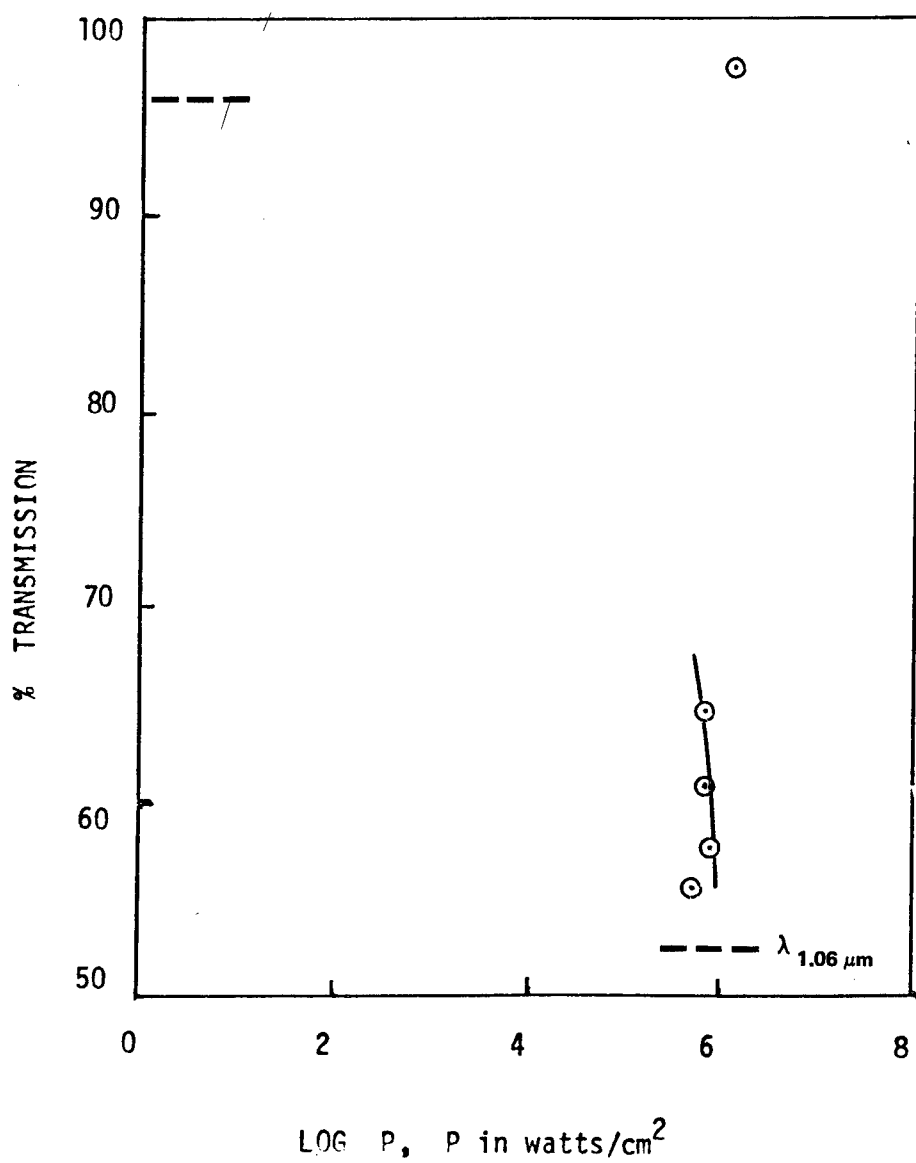


Figure 46. Optical saturation of NiDTAQ/DMF solution.

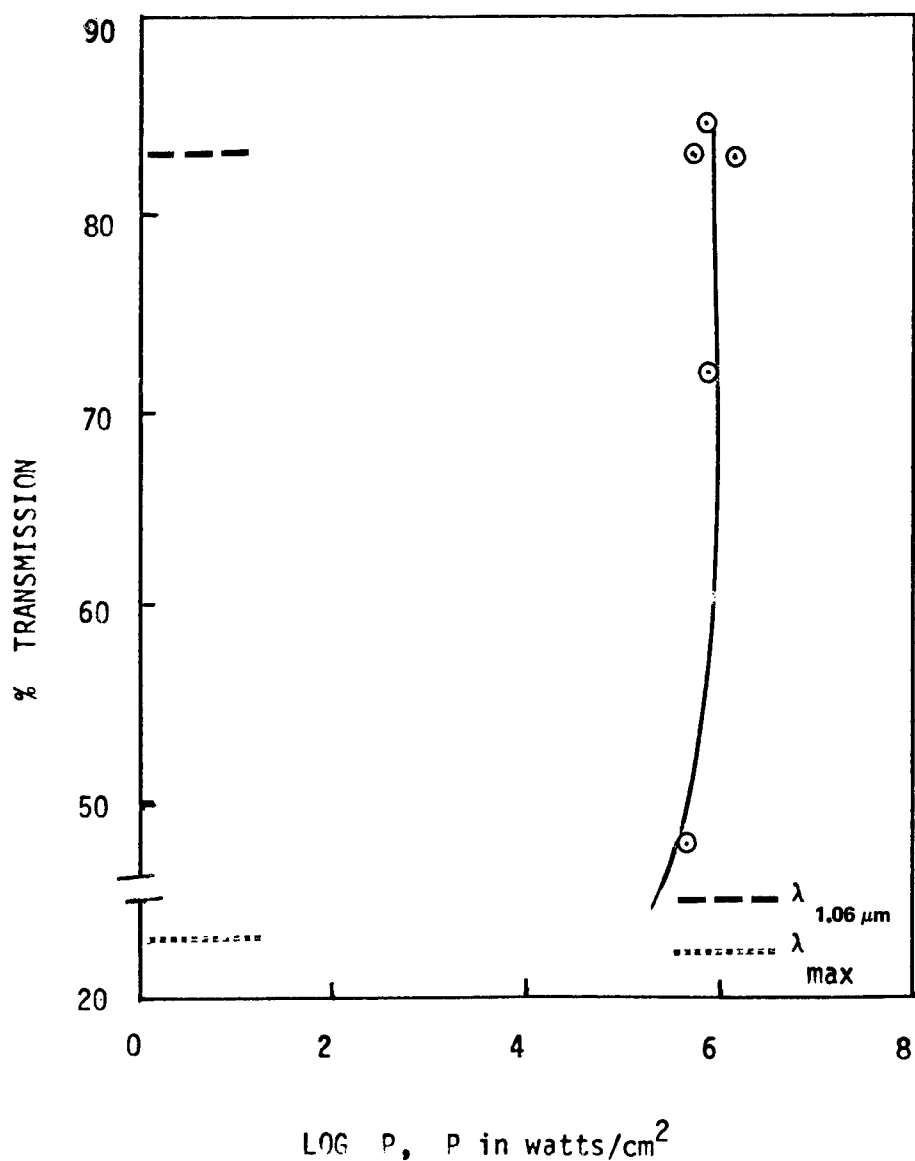


Figure 47. Optical saturation of NiTMD/DCE solution.

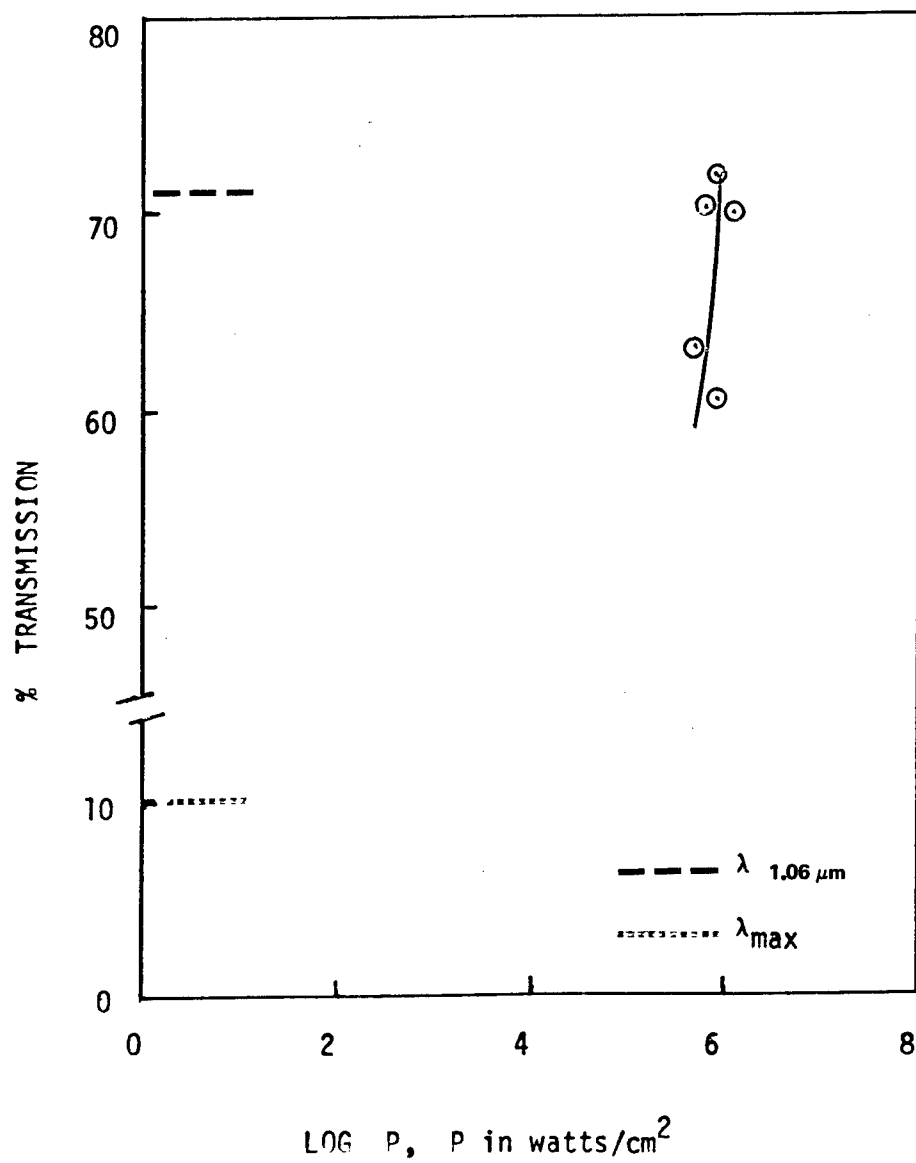


Figure 48. Optical saturation of PdTMD/DCE solution.

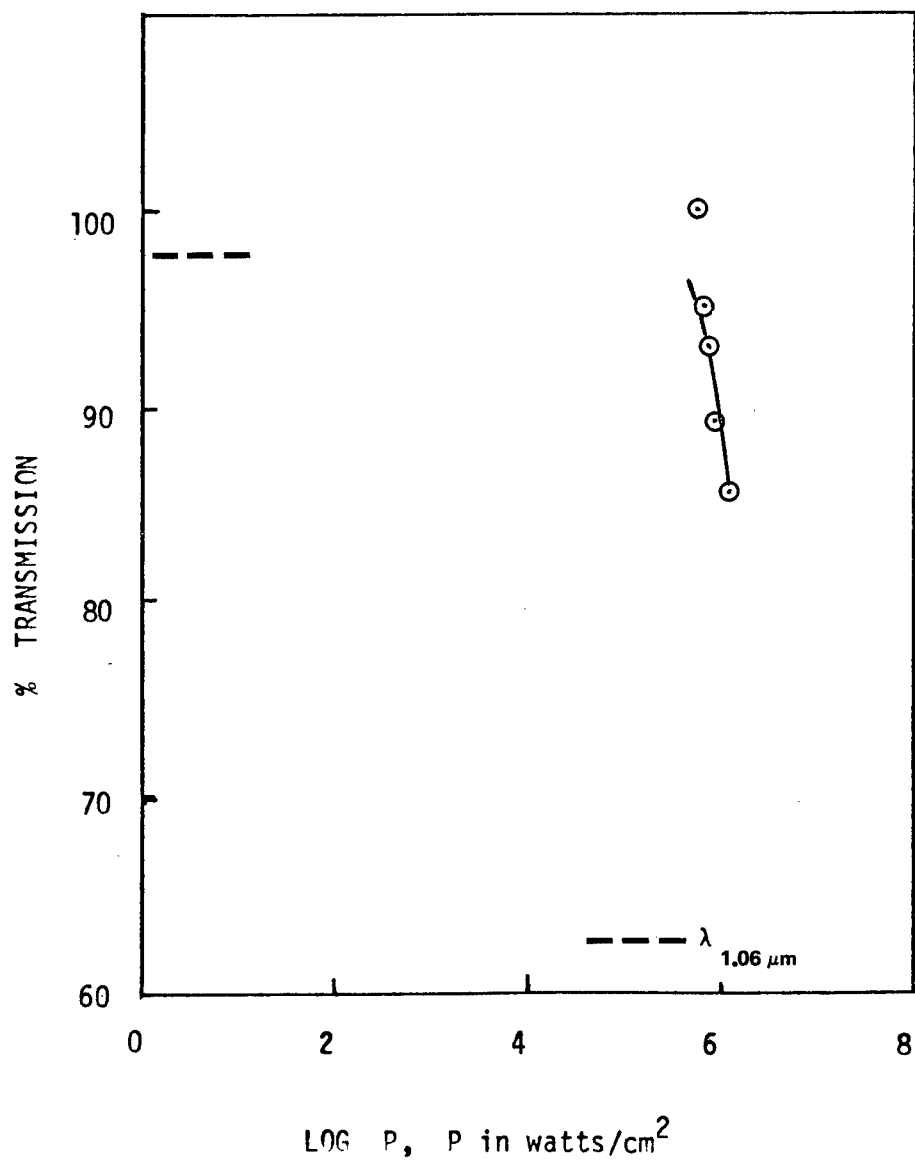


Figure 49. Optical saturation of PtTMD/DCE solution.

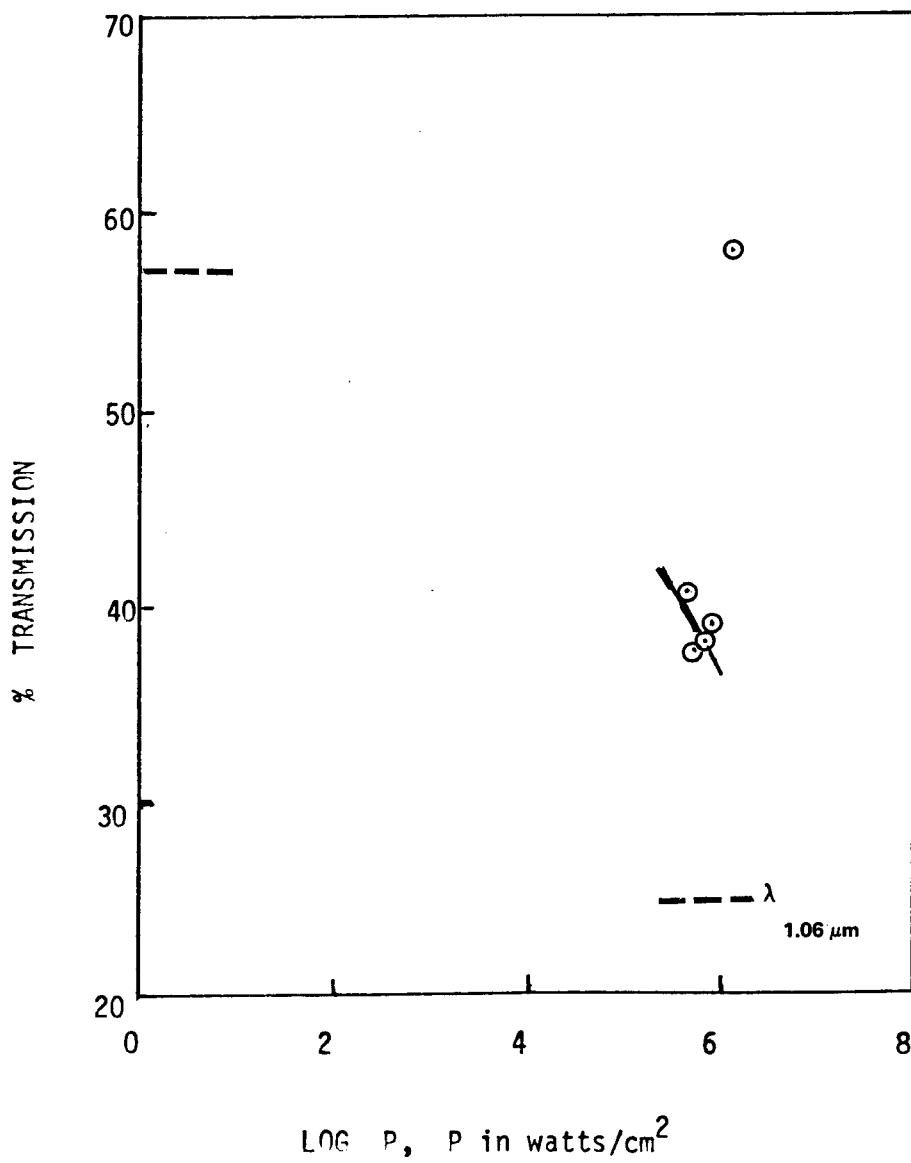


Figure 50. Optical saturation of NiDJG/DCE solution.

4. Passive Q-Switching of an Nd-Glass Laser for High-Energy Applications.

a. **Introduction.** An opportunity to use the Ni-DAD dye Q-switch in high-energy applications surfaced recently. Briefly, a requirement arose for a 5-joule giant pulse Nd laser. Results and implications are presented below for the initial studies done to meet the 5-joule giant pulse need. The results were obtained under a short time constraint and so cannot be regarded as a final evaluation.

b. **Experimental Apparatus.** Dye solutions in 1,2-dichloroethane were prepared as in paragraph 1 of this report. The absorbance of the Q-switch solution was about 0.3 in the work reported below, corresponding to a concentration of about 1.2×10^{-5} M (ϵ_{max} is 2.5×10^4 l-mol⁻¹-cm⁻¹ for this dye).⁹ The dye solutions were used in 1-cm path length absorption cells (1-in. diameter parallel faces) fabricated from Infrasil quartz.

The laser element used was a 6-in. by 1/2-in. O.D. neodymium silicate glass rod (Kigre Co.), in the experimental arrangement shown in Figure 51.²² The electro-optical Q-switch used was a KD*P Pockels Cell). Preliminary work was done with a ND:YAG laser, but rod damage prohibited reproducible results (note the dye Q-switch was not damaged).

III. RESULTS AND DISCUSSION

Results of the initial evaluation of the Ni-DAD dye Q-switch in high-energy lasers are summarized in Table 2. In Figure 52, our current results with the dye are presented with data for the dye reported earlier and with low-energy data obtained in this laboratory.^{10 23 24 25} Emphasis must be made here that no evidence of photochemical damage in the dye was observed as a consequence of these irradiations. Absorption readings taken before and after Q-switching were the same, within experimental error.

⁹ K. H. Drexhage and U. T. Muller-Westerhoff, IEEE J. of QE, QE-8 (9), 759 (1972).

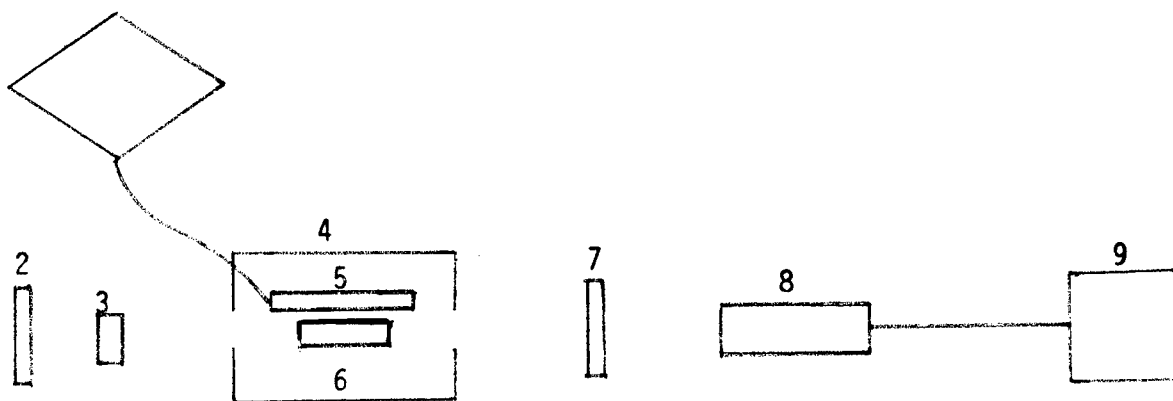
¹⁰ H. Lo, "Saturable Absorbing Materials for Q-Switching Neodymium Lasers," ECOM Research and Development Report ECOM-0122-F (May 1972).

²² W. Beattie and R. Tuttle, US Army (ERADCOM) private communication.

²³ S. A. Vasina, Yu M. Gryaznov, T. I. Kirsanova, V. K. Savelova, and R. E. Shamshin, Zh. Prikl. Spektrosk. 24(6), 794 (1976) (Eng).

²⁴ J. Stimpson, Korad, private communication.

²⁵ K. H. Drexhage and U. T. Mueller-Westerhoff, U.S. No. 3,743,964 (3 July 1973).



- LEGEND:
1. PFN, 50 μ f condenser and 50 μ H coil
 2. Rear mirror, 100% reflecting
 3. Q-switch, either absorption cell containing IBM dye, or Pockels cell (KD*P) and polarizer
 4. Laser cavity, close wrapped in aluminum foil
 5. Linear flashlamp, PEK XE-15
 6. Nd-silicate glass rod, $\frac{1}{2}$ " O.D. x 6" long
 7. Front mirror, either 75%, 50%, or 35% reflecting
 8. TRQ thermopile detector
 9. 150 μ V voltmeter (Keithley)

Figure 51. Diagram of apparatus used to generate and measure high-energy 1.06 μ m laser emission.

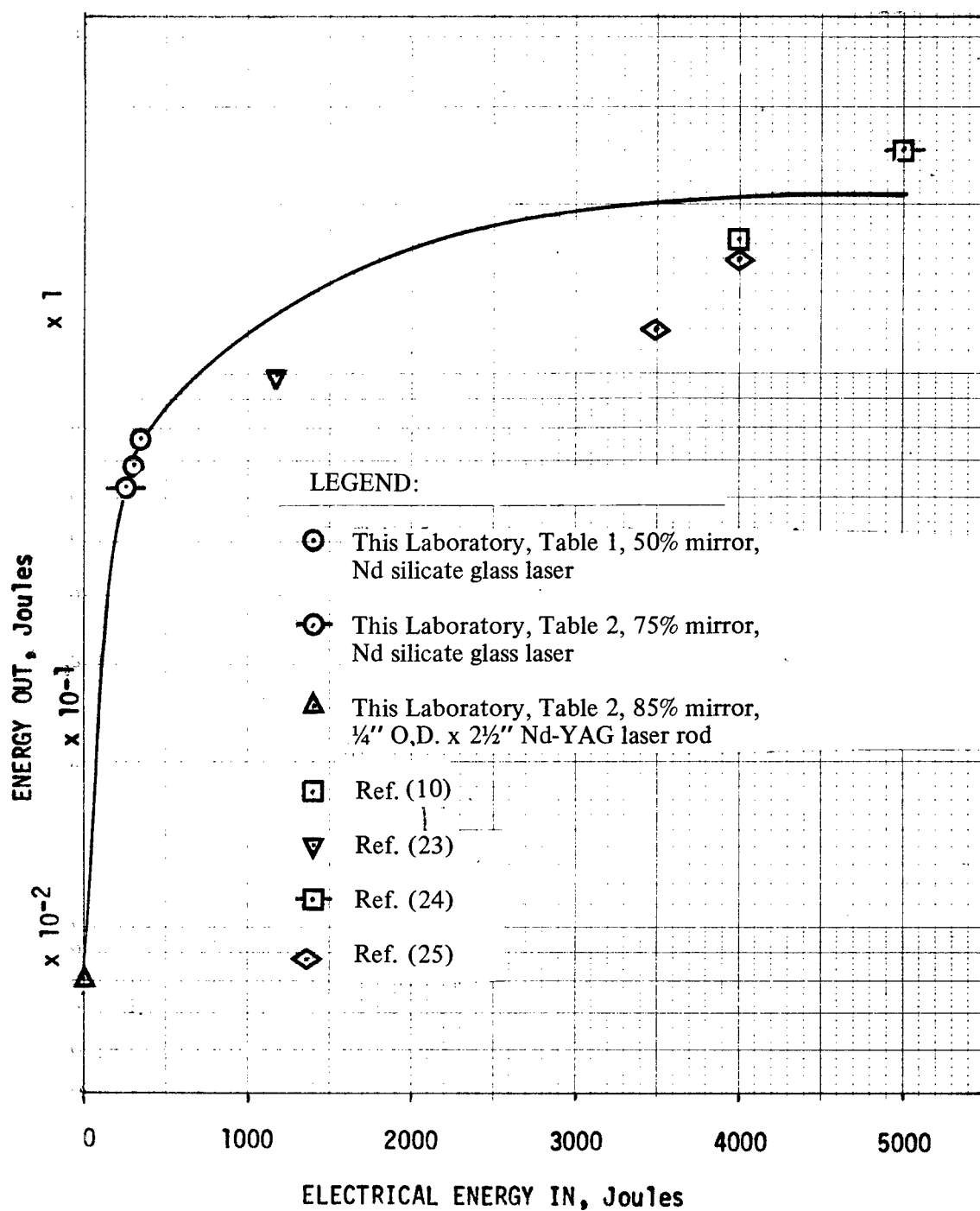


Figure 52. Apparent plateau of Ni-DAD response.

From Figure 52 and the summary of data given in Table 2, three major observations may be made, the hazards of extrapolation notwithstanding:

- a. The dye was a less efficient Q-switch than the Pockels Cell used.
- b. The dye Q-switch is capable of higher energy operation than that achieved in the present work.
- c. To achieve high-energy outputs with the dye Q-switch, higher input energies to the laser will be required (probable at least 2500 J electrical input for 2 J output).

The high-energy dye Q-switch data were obtained on a Nd-silicate glass rod, while the Pockels Cell data were achieved with a Kigre Q-88 Nd-phosphate glass rod. No data were available for the dye Q-switch with the phosphate rod, though one could assume the phosphate rod would withstand higher input energies. (The silicate rod showed evidence of damage at 10 J long pulse input.)²⁶ The data obtained here, as shown in Figure 52, cannot be said to represent the optimum match of dye Q-switch and Nd-glass (phosphate) laser, but the data from other sources indicated that a 2-3 J giant pulse could be attained with the Ni-DAD dye solution.^{5 25 27}

Equally relevant to the question of high-energy performance of this dye is the apparent low efficiency, particularly at higher input energies (Table 2). The fact that the absorbance at 1.06 μm remained the same before and after irradiation indicated no irreversible photochemical change was occurring. Further, no evidence of precipitation or color change was visible. From a molecular viewpoint, the multiplicity of energy levels available for population in the dye (Figure 3) suggests that at least one metastable excited state may be formed. The constancy of absorbance values indicates that this state decays to the ground state without reacting chemically.

⁵ K. Venkataraman, *The Chemistry of Synthetic Dyes*, Vol I, Academic Press Inc., New York, NY, 1952, Chap. VIII.

²⁵ K. H. Drexhage and U. T. Mueller-Westerhoff, U.S. No. 3,743,964 (3 July 1973).

²⁶ W. Beattie and R. Tuttle, US Army (ERADCOM) private communication.

²⁷ J. Stimpson, Korad, private communication.

For Q-switching to occur, the metastable state must be transparent to the laser frequency, and this state can be viewed as a "molecular trap" for excited molecules. Figure 2 is a diagram of this situation in its most simplistic form. The relaxation times from the metastable state to the ground state must be a governing factor in the efficiency of a dye Q-switch. For Ni-DAD dissolved in DCE, this lifetime has been measured and reported as 36 nanoseconds. (No strong radiative emission has been observed for this dye, so chiefly only non-radiative decay is involved).⁸ Relaxation times such as these are relatively longer than those from the primary (singlet) excited state and are sufficiently long to allow interaction with the (solvent) environment. Manipulation of the environment may be effective, therefore, in maximizing the output obtainable with a particular dye Q-switch. Unless an appreciable concentration or population of dye molecules is attained (in this "transparent" metastable state) in a time interval consistent with that of the laser pulse, Q-switching will be less efficient, or even unlikely. The effectiveness of "manipulating" the chemical environment of a dye molecule in the metastable excited state has already been accomplished with the ruby laser passive Q-switch, cryptocyanine, albeit at a low energy level. When a viscous solvent (glycerol) was used, enough cryptocyanine molecules were detained in the metastable state so that output energies were almost twice those obtained in a low viscosity solvent (propanol).^{17 18} Molecular structure of the solvent can affect relaxation time also. Variation in relaxation time is found for Ni-DAD to range from 9 nanoseconds in benzene to 0.22 nanoseconds in a heavy-atom solvent as iodomethane.⁸ Ni-DAD-solvent combinations should be evaluated for optical high energy performance.

Another factor may have reduced the apparent effectiveness of the Ni-DAD Q-switch. The radiation detector responds to a signal which is time-wavelength span-intensity dependent. Spectral narrowing due to hole-burning (evidenced by a lowering of the absorbance at a particular frequency, observed in absorption vs. frequency curves) may have occurred. Inhomogeneous broadening of the absorption band of a dye may be caused by variations in the molecular environment (as solvent cage or molecular configuration).²⁵ Such narrowing, along with associated frequency locking, has been observed for other passive absorbers.^{17 18 28 29 30 31} No such observations have been made to date for Ni-DAD. The wavelength span of the giant pulse was not determined here for the dye nor was it measured for the Pockels Cell. Though the pulse duration for the dye (75% mirror) was determined in our experimental configuration to be 33 nanoseconds, no value for the Pockels Cell was obtained. An explanation for the apparent relative inefficiency of the dye Q-switch may depend upon measurements of pulse duration and wavelength interval as well as intensity.

⁸ D. Magde, B. A. Bushaw, and M. W. Windsor, *Chem. Phys. Ltrs.* 28(2), 263 (1974).

¹⁷ M. L. Spaeth and W. R. Sooy, *J. Chem. Phys.* 48(5), 2315 (1968).

¹⁸ W. R. Sooy, et al., "Saturable Dye Optical Switch Investigation," US Army Electronics Command Technical Report ECOM-01237-F, Ft. Monmouth, NJ, December 1966.

²⁵ K. H. Drexhage and U. T. Mueller-Westerhoff, U.S. No. 3,743,964 (3 July 1973).

²⁸ G. Mourou, *IEEE J. of QE*, QE-11 (1), 1 (1975).

²⁹ M. Hercher, W. Chu and D. L. Stockman, *ibid.*, QE-4 (11), 954 (1968).

³⁰ C. R. Giuliano and L. D. Hess, *ibid.*, QE-3 (8), 358 (1967).

³¹ B. H. Soffer and B. B. McFarland, *Appl. Phys. Ltrs.*, 8 (7), 166 (1966).

Improved efficiency may be realized by optimizing the laser apparatus, the choice of solvent, and detector response. But more critical to the high energy applications of Ni-DAD is the apparent plateau in "energy out" values seen in Figure 52. Optical saturation studies performed at higher incident power densities than used in paragraph 3 would indicate whether opening is complete or incomplete for the dye. Figure 36 for Ni-DAD/DCE shows opening up to 80 percent transmission, at a power density of 1.5 MW/cm^2 . Optical saturation studies done elsewhere with Ni-DAD/DCE (33 percent transmission initially) and a neodymium glass laser (8 x 120 mm rod, 40 percent reflecting mirror) did show a plateau (or incomplete opening) at about 70 percent transmission with power densities between 5 and 60 MW/cm^2 .²³ No leveling-off even at 80 percent transmission was found in our optical saturation curves, using a Nd:YAG laser and an 85 percent reflecting mirror. We did not use such high power densities, however. In that same study, a maximum energy of 1 J was obtained for the dye Q-switched output, which is much less than the 2.5 J reported by others.³² One can conclude that there is a limiting value for the energy output for a neodymium laser Q-switched with Ni-DAD. What has not been established is the maximum value of that limit, since laser configuration variables, as well as Q-switch composition, affect the output.

IV. CONCLUSIONS

Fifteen new dithiene complexes have been tested as dye Q-switches for the neodymium-YAG laser. Seven of these complexes succeeded in Q-switching the laser. One complex, Ni-ODD, approached the well known dye Q-switch, Ni-DAD, in energy output and stability. KBr was not found to be a successful dye Q-switch host material though good optical quality specimens were not achieved. Optical saturation studies showed "opening" of the dyes which were successful Q-switches. As new near-infrared absorbing dithiene complexes are developed through molecular engineering techniques, optical saturation techniques will be useful for evaluating their potential as Q-switches. Dithienes with absorption maxima ranging from $0.86 \mu\text{m}$ to $1.28 \mu\text{m}$ have been treated in this report.

Evaluation of the available data on high energy applications of the Ni-DAD dye Q-switch indicate that the optimum performance of this dye Q-switch has not been realized. Its performance was not limited by photochemical instability. Better results may be expected with a Nd-phosphate glass laser rod. Use of a viscous solvent might have been beneficial, also. To accurately compare the performances of the KD*P Pockels Cell and Ni-DAD, measurements of both the laser pulse duration and the emission spectrum are needed. Evidence exists for a high energy plateau in the output of a Ni-DAD Q-switched neodymium laser, but the maximum value for such a level remains to be determined.

²³ S. A. Vasina, Yu M. Gryaznov, T. I. Kirsanova, V. K. Savelova, and R. E. Shamshin, *Zh. Prikl. Spektrosk.* 24(6), 794 (1976) (Eng.).

³² J. Stimpson, Korad, private communication.

DISTRIBUTION FOR NV&EOL REPORT DELNV-TR-0031

No. Copies	Addressee	No. Copies	Addressee
2	Commander ERADCOM (DRDEL-CP-C) 2800 Powder Mill Road Adelphi, MD 20783	1	Project Manager TOW/DRAGON Redstone Arsenal, AL 35809
1	Director Atmospheric Sciences Lab ATTN: DELAS-D White Sands Missile Range, NM 88002	1	Project Manager GLLD/LTD Redstone Arsenal, AL 35809
1	Director CS&TA Laboratory ATTN: DELCS-D Fort Monmouth, NJ 07703	1	Project Manager VIPER/AHAMS Redstone Arsenal, AL 35809
1	Director Electronic Warfare Lab ATTN: DELEW-D Fort Monmouth, NJ 07703	1	Project Manager AAH AVARADCOM St. Louis, MO 63166
1	Director Electronics Technology & Devices Laboratory ATTN: DELET-D Fort Monmouth, NJ 07703	1	Project Manager TADS/PNVS AVARADCOM St. Louis, MO 63166
1	Commander Harry Diamond Labs ATTN: DELHD-AC Adelphi, MD 20783	1	Commander ARRCOM ATTN: DRSAR-CPE Rock Island, IL 61299
1	Director Signal Warfare Lab ATTN: DELSW-D Vint Hill Station, VA 22186	1	Project Manager RPV AVARADCOM St. Louis, MO 63166
1	Project Manager XM-1 Tank System Warren, MI 48090	27	Commander CERCOM ATTN: DRSEL-CP-CR (C. Pearce) Fort Monmouth, NJ 07703
1	Project Manager M60 Tank System Warren, MI 48090	3	Commander AFSC/ACC Andrews AFB, MD 20334

No. Copies	Addressee	No. Copies	Addressee
1	Project Manager MICV Warren, MI 48090	1	Director Defense Advanced Research Project Agency Rosslyn, VA 22209
1	Commander MIRADCOM ATTN: DRDMI-DC Redstone Arsenal, AL 35809	1	Commander MERADCOM ATTN: DRDME-CA Fort Belvoir, VA 22060
1	Commander MIRCOM ATTN: DRSMI-FO Redstone Arsenal, AL 35809	1	Commandant Defense Systems Management School Fort Belvoir, VA 22060
1	Commander AVARADCOM ATTN: DRCV-BC St. Louis, MO 63166	1	Commander US Army Engineer School Fort Belvoir, VA 22060
1	Commander TSARCOM ATTN: DRSTS-CO St. Louis, MO 63166	1	Commander US Operational Test and Evaluation Agency 5600 Columbia Pike Falls Church, VA 22041
1	Commander TARADCOM ATTN: DRCTA-VC Warren, MI 48090	1	Commander USACSC Fort Belvoir, VA 22060
1	Commander TARCOM ATTN: DRSTA-NC Warren, MI 48090	1	HQDA ATTN: DACA-CA Washington, DC 20310
1	Commander NARADCOM ATTN: DRDNA-O Natick, MA 01760	12	Defense Documentation Center ATTN: DDC-TCA Cameron Station (Bldg 5) Alexandria, VA 22314
1	Commander AMMRC Watertown, MA 02172	1	Commander US Army Training & Doctrine Command ATTN: ATCD-AN Fort Monroe, VA 23651
1	Commandant US Army Infantry School Fort Benning, GA 31905	2	Commander US Army Logistics Center Fort Lee, VA 23801

No. Copies	Addressee	No. Copies	Addressee
1	Commander US Army Systems Analysis Agency Aberdeen Proving Ground, MD 21005	1	Commandant US Army Armor School Fort Knox, KY 40121
1	Commander US Naval Research Lab Washington, DC 20375	1	Commandant US Army Field Artillery School Fort Bliss, TX 79916
1	Commander HQ DARCOM ATTN: DRCDE-DE Alexandria, VA 22333	1	Study Center National Maritime Research Center King's Point, NY 11024
1	Director ATTN: DELNV-TMS/SEMCO Fort Belvoir, VA 22060	1	Commander USAAVNC Ft. Rucker, AL 36362
1	Project Manager REMBASS ATTN: DRCPM-RBS Fort Monmouth, NJ 07703	1	Commander ESD/ACC Hanscomb AFB, MA 01730
1	Project Manager FIREFINDER ATTN: DRCPM-FF Fort Monmouth, NJ 07703	1	Commander US Naval Ordnance Lab/White Oak ATTN: Technical Library Silver Spring, MD 20910
1	Department of Defense Production Engineering Spt Ofc (PESO) ATTN: D. Anderson Cameron Station Alexandria, VA 22314	1	Commander Naval Electronics Lab Ctr ATTN: Library San Diego, CA 92152
1	Project Manager CAC ATTN: DRCPM-CAC Vint Hill Station, VA 22186	1	Armament Development and Test Center ATTN: DLOSL, Tech Library Eglin Air Force Base, FL 32542
1	Project Manager SOTAS ATTN: DRCPM-STA Ft. Monmouth, NJ 07703	3	Director NV&EOL ATTN: DELNV-L (R. Buser) Fort Belvoir, VA 22060
		1	Commander Sacramento Army Depot Sacramento, CA 95813

No. Copies	Addressee
1	Commander Anniston Army Depot Anniston, AL 36201
1	Commandant US Army Air Mobility R&D Ctr Ames Research Center Moffett Field, CA 94035
1	Commander New Cumberland Army Depot New Cumberland, PA 17070